Supplemental Information for:

The bacterial cell-cycle regulator GcrA is a σ^{70} co-factor that drives gene expression from a subset of methylated promoters

Diane L. Haakonsen, Andy H. Yuan, and Michael T. Laub

Content:

Supplemental Figure Legends

Figure S1. Controls for ChIP-Seq experiments. (A) Abundance of GcrA and GcrA-3xFLAG was assessed by immunoblotting with a polyclonal GcrA antibody. Serial three-fold dilutions are shown. RpoA is a loading control. Morphology of the indicated strains grown to exponential phase was examined via phase microscopy. (B) Scatterplot of ChIP-Seq signals for two GcrA-3xFLAG strains (Δ*gcrA,* P_{xyl}-*gcrA-3xFLAG* grown in PYE + xylose) and (P_{gcra}-*gcrA-3xFLAG* grown in PYE) at σ^{70} promoters with normalized σ^{70} signal > 0.1 (N=450). (C) ChIP-Seq profiles of GcrA (red) (Δ*gcrA,* P_{xyl}-*gcrA-3xFLAG* grown in PYE + xylose) and untagged GcrA (black) (Δ*gcrA,* P_{xyl}-*gcrA* grown in PYE + xylose) both immunoprecipitated with an anti-FLAG antibody. (D) Scatterplot of ChIP-Seq signals for GcrA (Δ*gcrA,* P_{xyl}-*gcrA-3xFLAG* grown in PYE + xylose) and σ^{70} (wild-type grown in PYE) at σ^{70} promoters with normalized σ^{70} signal > 0.1 (N=450). (E) Scatterplot of ChIP-Seq signals for RNAP (*rpoC::rpoC-3xFLAG* grown in PYE) and σ^{70} (wild-type grown in PYE) at σ^{70} promoters with normalized σ^{70} signal > 0.1 (N=450). (F) Rifampicin-treated and untreated ChIP-Seq signals for GcrA and σ^{70} at two promoters that are not bound in untreated condition. The two genomic regions are schematized at the bottom with vertical black lines indicating locations of GANTC methylation sites.

Figure S2. GcrA does not interact with other *Caulobacter* sigma factors; a region of domain 2 in σ^{70} interacts with GcrA. (A) Bacterial two-hybrid analysis of the interaction between GcrA and the 16 predicted alternative *Caulobacter* sigma factors is shown. The number on top of each column is the CCNA gene number of the sigma factor tested. (B) Alignment of domain 2 of *Caulobacter* and *E. coli* σ^{70}. Chimera composition is given below the alignment with blue for *Caulobacter* and red for *E. coli.* The same color scheme is shown on the *E. coli* crystal structure of domain 2 (4LK1) (Bae et al. 2013). N and C termini are labeled on the crystal structures. Bacterial two-hybrid analysis of the interaction between GcrA and domain 2 of σ^{70} from *Caulobacter*, *E. coli,* and chimeras 1 and 2. (C) Western blot using anti-FLAG antibody for variants of GcrA-3xFLAG after 2 hour induction with 0.3% xylose; related to (Fig. 2G). FL is for full-length, E is the empty vector.

Figure S3. *In vitro* filter binding assay for methylated probes; enrichment of methylation sites at σ^{70} promoters. (A) Scatterplot of ChIP-Seq signals for GcrA (Δ*gcrA,* P_{xyl}-*gcrA-3xFLAG* grown in PYE + xylose) and σ^{70} (wild-type grown in PYE) at σ^{70} promoters. Promoters with at

least one methylation site within 40 bp of the transcription start site are shown in blue, the rest are in black. (B) *In vitro* GcrA binding affinity measured by filter binding for the probes (each ~160-200 bp) indicated. The average for three replicates with SD is shown. The P_{mipZ} panel includes the same data in Fig. 3D for comparison. Sequences surrounding the methylation sites in P_{mipZ} and P_{ftsZ} and their ranks are indicated. (C) The ChIP signals for GcrA, RNAP and σ^{70} from rifampicin-treated cells at the *mipZ* and *ftsZ* promoters. The transcriptional start sites are shown for reference. Methylation sites positions (given by middle N of NGANTCN) are indicated with a vertical line (P_{mipZ}: site ranked 12th is at +4 and site ranked 3rd is at +12 ; $P_{ftsZ:}$ site ranked 3rd is at -21 and site ranked #22 is at -73). (D) Ranking of the 32 NGANTCN sequences based on the average ChIP enrichment of GcrA at all non-promoter regions harboring each sequence; also see Fig. 3C. (E) GcrA binding curves for the probes indicated: methylated P_{cckA}, unmethylated P_{cckA}, and methylated P_{cckA} mutated to have low-ranking methylation sites, P_{cckA}(LM). Sequences surrounding the methylation sites in P_{cckA} and P_{cckA}(LM) and their ranks are indicated. Location of transcription start site is given for reference, methylation site ranked 3rd is at +13. The average for three replicates with SD is shown. (F) Histograms of the GcrA:σ^{70} ChIP ratios at σ^{70} promoters. Ratios were computed at all transcription start sites mapped with σ^{70} signal > 6 rpm.

Figure S4. Kinetic analysis of open complex formation by RNAP holoenzyme and GcrA on the *cckA* promoter. Multiple-round *in vitro* transcription from the methylated *mipZ* promoter using the indicated probe (right). Methylation sites positions (given by middle N of NGANTCN) are indicated with a vertical line (site ranked 12th is at +4 and site ranked 3rd is at +12). Probe 2 is the same probe used in Fig. 4.

Figure S5. GcrA affects expression of cell division genes. (A) Histogram of the GcrA:σ^{70} ChIP ratios at σ^{70} promoters in rifampicin-treated cells. A normal distribution (blue) was fitted to the left side of the histogram and the threshold $2^{-0.5}$ used to define a high GcrA:σ^{70} ratio shown in red. (B) Representation of the overlap between the GcrA regulon promoters and promoters that are induced at the swarmer-to-stalk transition and down-regulated in GcrA-depleted cells. Swarmer-to-stalked cell regulated promoters were identified as described in the supplemental Materials and Methods. (C) Gene expression for the CtrA regulon in GcrA-depleted cells / wild-

type cells at three cell-cycle timepoints. (D) Gene expression for known cell division genes in GcrA-depleted cells / wild-type cells at three cell-cycle timepoints.

Figure S6. Ectopic induction of *ftsZ* or *ftsN* does not complement a GcrA depletion. (A) Representative time-lapse images of wild-type and GcrA-depleted cells with TetR-mCerulean-labeled origins of replication; see Fig. 6C for summary data. (B) Growth of the *gcrA* depletion strain harboring the additional plasmids indicated, assessed by 10-fold serial dilutions on PYE xylose (to induce expression from plasmids) plates +/- vanillate. (C) Growth curve of a *gcrA* depletion strain (Δ*gcrA*, P_{van}-*gcrA*). Cells were washed 3 times in PYE prior to release in PYE +/- vanillate. (D) Western blot for GcrA and RpoA during a GcrA depletion (Δ*gcrA*, P_{van}-*gcrA*). Cells were washed 3 times in PYE prior to release in PYE and samples were taken at the indicated timepoints. (E) Western blot for GcrA and RpoA (loading control) for the strains tested in Fig. 6A. (F) Representative time-lapse images of *pstS::Tn5* and GcrA-depleted *pstS::Tn5* cells with TetR-mCerulean-labeled origins of replication. (G-H) Normalized histogram of times between successive replication initiations (G) and times between replication and division (H) in wild-type and GcrA-depleted cells. Median values are listed above.

Supplemental Materials and Methods

Bacterial strains and growth conditions

All strains used are listed in Table S4. *Caulobacter* strains were grown in PYE (rich medium) at 30 °C unless otherwise noted. Induction from the P_{xyl}, P_{van}, and P_{lac} promoters was achieved by supplementing media with xylose (0.3%), vanillate (500 μM), or IPTG (1 μM), respectively. Antibiotics were used at the following concentrations (liquid /plates): oxytetracycline (1 μg mL^{-1} / 2 μg mL^{-1}), spectinomycin (25 μg mL^{-1} / 200 μg mL^{-1}), kanamycin (5 μg mL^{-1} / 25 μg mL^{-1}), gentamycin (NA / 5 μg mL^{-1}). *E. coli* strains were grown in LB medium at 37 °C unless otherwise indicated; when necessary, media were supplemented with the following antibiotic concentrations (liquid/plates): kanamycin (30 μg mL^{-1} / 50 μg mL^{-1}), spectinomycin (50 μg mL^{-1}), oxytetracycline (12 μg mL^{-1}), gentamycin (15 μg mL^{-1} / 20 μg mL^{-1}), carbenicillin (50 μg mL^{-1} / 100 μg mL^{-1}).

Strain and plasmid construction

Strain construction: All plasmids and primers used are listed in Tables S5 and S6, respectively. Deletions were constructed via a two-step recombination method using *sacB* as a counter-selection marker (Skerker et al. 2005). Strain ML2296, a P_{xyl}-*gcrA* depletion strain, was constructed by first electroporating plasmid pMT585-*gcrA* into CB15N and selecting on kanamycin plates for integration at the xylose locus. The site of integration was confirmed by PCR using primers Rec-Uni and RecXyl-2 (Thanbichler et al. 2007). Next, plasmid pNPTS-spec-UP-tet-DW(*gcrA*) was introduced by electroporation and first integrants at the *gcrA* locus were selected on spectinomycin, tetracycline, and kanamycin. A second recombination step to select for plasmid excision was performed by growing first integrants overnight in PYE containing xylose and kanamycin. 1 μL of the overnight culture was plated on sucrose, tetracycline, and xylose. Sucrose resistant clones were restreaked to test for loss of spectinomycin resistance, indicative of plasmid excision, on plates containing spectinomycin and xylose. Clones were further verified by PCR using primers OL69 and OL70, which anneal outside the homology region found on the plasmid.

Strains ML2297 and ML2302 were constructed by transducing Δ*gcrA(*tet^R*)* from ML2296 into a strain containing pMT585-*gcrA-3xFLAG* integrated at the xylose locus or pMT552-*gcrA*

integrated at the vanillate locus, and selecting on tetracycline + xylose or tetracycline + vanillate, respectively. Phage transductions were performed as previously described (Ely 1991). ML2305 was constructed similarly by transducing Δ*gcrA(spec^R)* from LS3707 into a strain containing pMT644-*gcrA* integrated at the vanillate locus and selecting on spectinomycin + vanillate. All transductants were verified by PCR using primers OL69 and OL70.

Strains ML2298, ML2299, ML2300, ML2301, and ML2315 were constructed via single recombination and kanamycin selection with electroporated plasmids pNPTS138-*gcrA-3xFLAG,* pNPTS138-*rpoC-3xFLAG,* pNPTS138-*rpoH-3xFLAG,* pNPTS138-*rpoN-3xFLAG,* and pNPTS138-*rpoC-His$_{10}$*, respectively. All resulting clones were verified by PCR with a primer annealing outside the homology region found on the plasmid and a primer annealing to the FLAG or His_{10} tag coding sequence.

Strains ML2475, ML2476, ML2477 were constructed via single recombination and kanamycin selection with electroporated plasmids pNPTS138-*P$_{mipZ}$-venus,* pNPTS138-*P$_{mipZ}$(LM)-venus and* pNPTS138-*P$_{mipZ}$(NM)-venus*, respectively. All resulting clones were verified by PCR with a primer annealing outside the homology region to CCNA_02236 found on the plasmid and a primer annealing to the Venus coding sequence.

Strain ML2303 (kind gift of C. Aakre), a *spoT* deletion strain, was constructed via two-step recombination. First integrants of the pNPTS-138-Δ*spoT* integration vector were selected on kanamycin. A second recombination step to select for plasmid excision was performed by growing first integrants overnight in PYE. 1 μL of the overnight culture was plated on sucrose and sucrose resistant clones were restreaked to test for loss of kanamycin resistance, indicative of plasmid excision. Clones were further verified by PCR using primers (CAP173-CAP174) annealing outside the homology region found on the plasmid. Strain ML2304 was obtained by two successive transductions of *P$_{van}$-gcrA*(*kan^R*) from ML2302 and Δ*gcrA(spec^R)* from ML2305 followed by transformation of the plasmid pMR20-P$_{lacI}$-*lacI*-P$_{lac}$-*spoT(H67A)*.

Strain ML2316 was constructed by transduction of *pstS::Tn^5* (YB767) into ML2305.

Strain ML2317 (kind gift of C. Aakre) was constructed by transduction of the *Cori::tetO(gent^R)* from strain ML1678 and two-step integration of the pNPTS138-hfaAUP-P$_{lacI}$-*lacI*-P$_{lac}$-tetR-mCerulean-hfaADW integration vector at the *hfaA* locus. Strain ML2318 was constructed by

integration of P_{van}-*gcrA(rif^R)* (pMT561-*gcrA*) at the vanillate locus in strain ML2317 followed by transduction of Δ*gcrA(tet^R)* from ML2302. Strains ML2319 and ML2320 were constructed by transduction of *pstS::Tn^5* (YB767) into ML2317 and ML2318, respectively.

Strains ML2306-ML2314 were constructed by electroporation of the appropriate pMT375 variant (see Table S5) into ML2305 and selection on tetracycline, spectinomycin, and vanillate. All bacterial two-hybrid strains (ML2321-ML2369) were obtained by co-transformation of the appropriate plasmid pairs into *E. coli* BTH101 with selection on kanamycin and carbenicillin. All strains for protein expression and purification (ML2370-ML2378) were generated by electroporation of the appropriate plasmids into BL21DE3 pLysS cells.

Integration plasmids: The pNPTS-spec-UP-tet-DW(*gcrA*) integration vector was constructed by amplifying homology regions upstream and downstream (~600 bp) of the *gcrA* coding sequence using primer pairs OL3_up_gcrA_F, OL4_up_gcrA_R and OL5_dw_gcrA_F, OL6_dw_gcrA_R. The tetracycline (*tet*) resistance cassette was amplified from template pKO3 using primer pair OL7_tet_F, OL8_tet_R. The upstream homology fragment was fused to the *tet* cassette by SOE-PCR using primers OL3_up_gcrA_F and OL8_tet_R. This PCR product was then fused to the downstream homology region by SOE-PCR using primers OL3_up_gcrA_F and OL6_dw_gcrA_R. The resulting PCR product was cloned into the pENTR vector using the pENTR/D-TOPO cloning system (Life Technologies) and then recombined into the pNPTS-spec-DEST vector.

The pNPTS138-*gcrA-3xFLAG* integration vector to introduce a 3xFLAG tag at the C-terminus of the *gcrA* coding sequence was constructed by amplifying a homology region of the C-terminus of *gcrA* (~500 bp) using primer pair GcrA-3xFLAGSOE-CTERM-R, HindIII-GcrActerm3xFLAG_F. This PCR product was fused to the 3xFLAG coding sequence using primers HindIII-GcrActerm3xFLAG_F and 3xFLAG-SACI-R, and then amplified with primers 3xFLAG-F, 3xFLAG-SACI-R. The resulting product was digested with HindIII and SacI and cloned into the pNPTS138 vector digested with the same enzymes. The pNPTS138-*rpoC-3xFLAG, pNPTS138-rpoH-3xFLAG* and *pNPTS138-rpoN-3xFLAG* plasmids were constructed using the same strategy (~700 bp homology region) with primer pairs (rpoC-HindIII-Cterm-F, Rev-rpoC3xFlag), (rpoH-HindIII-3x-F, rpoH-3x-Flag-R), and (RpoN-HindIII-3x-F, rpoN-3x-R), respectively, and (3xFLAG-F, Rev-3xFlag-EcoRI) for 3xFLAG amplification and cloned using

HindIII and EcoRI restriction sites. The *pNPTS138-rpoC-His$_{10}$* was constructed by two consecutive PCR reactions using primers rpoC-HindIII-Cterm-F, rpoC-R1linker and then primers rpoC-HindIII-Cterm-F, rpoC-R2linker-10His) followed by cloning into pNPTS138 using the HindIII and EcoRI restriction sites.

The pNPTS138-*P$_{mipZ}$-venus,* pNPTS138-*P$_{mipZ}$(LM)-venus and* pNPTS138-*P$_{mipZ}$(NM)-venus* integration vectors to introduce reporter genes for wild-type and mutant *mipZ* promoters near the endogenous *mipZ* locus were constructed by amplifying a homology region for the CCNA_02236 gene using primer pair 2236-F-HindIII and 2236-R-fuse-mipZ. This was then fused by SOE-PCR to the *mipZ* promoter sequence (or mutant *mipZ* promoter sequence, see DNA probe construction for details on how the mutations were introduced) amplified with primer pair FB-mipz-F and PmipZ-R-fuse-Venus and to the *Venus* coding sequence amplified with primers Venus-F and Venus-R-NheI. The resulting fragment was cloned using HindIII and NheI restriction sites into pNPTS138.

The pNPTS138-Δ*spoT* integration vector (C.Aakre) was constructed by amplifying homology regions upstream and downstream (~600 bp) of the *spoT* coding sequence using primer pairs (CAP133, CAP134) and (CAP135, CAP136) followed by SLIC cloning into pNPTS138 digested at the HindIII and EcoRI restriction sites.

Plasmids pMT585-*gcrA*, pMT552-*gcrA*, pMT644-*gcrA* and pMT561-*gcrA* were generated by cloning the PCR product amplified by primers OL17_NdeI_gcrA_F, OL18_SacI_gcrA_R and digested with NdeI and SacI into the digested vectors pMT585, pMT552, pMT644 and pMT561, respectively. The plasmid pMT585-*gcrA-3xFLAG* was constructed similarly except with the final PCR product obtained from SOE-PCR amplification of the *gcrA* coding sequence using primers OL17_NdeI_gcrA_F and GcrA-3xFLAGSOE-CTERM-R, and the 3xFLAG coding sequence using primers 3xFLAG-F and 3xFLAG-SACI-R. All plasmids were sequence verified.

The pNPTS138-hfaAUP-P$_{lacI}$-*lacI*-P$_{lac}$-tetR-mCerulean-hfaADW integration vector (C.Aakre) was constructed by SLIC cloning into pNPTS138 digested with HindIII and EcoRI of three PCR fragments, 600 bp upstream of the hfaA locus, the P$_{lacI}$-*lacI*-P$_{lac}$-tetR-mCerulean and 600 bp downstream of the hfaA locus amplified with primer pairs (CAP94, CAP95), (CAP96, CAP140) and (CAP139, CAP99), respectively. The P$_{lacI}$-*lacI*-P$_{lac}$-tetR-mCerulean PCR fragment was

constructed by successive rounds of SOE-PCR with PCR fragments P_{lacI}-*lacI*-P_{lac} (CAP96, CAP137), tetR (CAP138, CAP60) and mCerulean (CAP61, CAP140).

Replicative plasmids: All pMT375-based plasmids were constructed using restriction sites NdeI and SacI. PCR products cloned into pMT375-*ftsN*, pMT375-*ftsZ,* pMT375-*gcrA,* were amplified with the following primer pairs: (FtsN-NdeI-F, FtsN-SacI-R), (NdeI-FtsZ-F, FtsZ-R-SacI), (OL17_NdeI_gcrA_F, OL18_SacI_gcrA_R), (OL17_NdeI_gcrA_F, GcrA-Nterm-R321-SacI), and (GcrA-Cterm-151-F-NdeI, OL18_SacI_gcrA_R), respectively. pMT375-$gcrA_{1\text{-}107}$*_3xFLAG,* and pMT375-$gcrA_{51\text{-}173}$-*3xFLAG* were constructed by a first amplification with the following primers (OL17_NdeI_gcrA_F, NL-fuse3Xflag), and (GcrA-Cterm-151-F-NdeI, GcrA-3xFLAGSOE-CTERM-R) followed by SOE-PCR eith the 3xFLAG fragment as described above for integration plasmids.

The plasmid pCT133-P_{lacI}-*lacI*-P_{lac}-*spoT(H67A)* (kind gift of C.Aakre) was constructed in three steps. First, the plasmid pENTR-P_{lacI}-*lacI*-P_{lac}-*spoT* was obtained by SLIC cloning with PCR fragments amplified with primer pairs (CAP66, CAP391 using *E. coli* DNA as template) and (CAP392, CAP393) and a modified pENTR vector containing a multiple cloning site digested with XmaI and EcoRI. Second, site-directed mutagenesis was performed on pENTR-P_{lacI}-*lacI*-P_{lac}-*spoT* to introduce the H67A mutation using primer pair CAP394 and CAP395. Third, pENTR-P_{lacI}-*lacI*-P_{lac}-*spoT(H67A)* was recombined into pCT133.

All bacterial two-hybrid plasmids were cloned using XbaI and KpnI restriction sites to introduce coding regions of interest. The PCR product to clone Chimera 1 of *Caulobacter* and *E. coli* domains 2 of σ^{70} (Fig. S2B) was constructed by successive rounds of SOE-PCR with PCR fragments amplified with primer pairs (sig70nt319-F, CC-159-R-fuse-EC139; *Caulobacter* DNA template), (EC139-F, EC349-R; *E. coli* DNA template) and (CC-390-F-fuse-EC349, rpoDaa484-R; *Caulobacter* DNA template). The PCR product to clone Chimera 2 of *Caulobacter* and *E. coli* domains 2 of σ^{70} (Fig. S2B) was constructed by successive rounds of SOE-PCR with PCR fragments amplified with primer pairs (89Ec-F-XbAI, EC138-R; *E. coli* DNA template), (CC-160-F-fuseEC138, 389CCfuse350EC-R; *Caulobacter* DNA template) and (350Ec-F, EC444-R-KpnI; *E. coli* DNA template).

All pET28b-based vectors containing *gcrA* variants were cloned using the PCR products used to generate pMT375 plasmids. pET28b-His$_6$-*rpoD,* pET28b-*His$_6$-rpoH,* pET28b-His$_6$-*rpoN and pET28b-His$_6$-ccrM* were constructed by PCR amplifying with primer pairs (RpoD-pet28-NdeI-F, rpoD-pet28-HindIII-R), (rpoH-pet28-NdeI-F, rpoH-pet28-HindIII-R), (rpoN-pet28-NdeI-F, rpoN-pet28-HindIII-R) and (ccrm-NdeI-F, ccrm-EcoRI-R). pGEX-4T2-GcrA was cloned by PCR amplification of the *gcrA* coding sequence with (F-GcrA-BamHI, R-GcrA-SalI) and ligated into pGEX-4T2 (kind gift of D. Barthelme).

Chromatin Immunoprecipitation Sequencing (ChIP-Seq)

Bacterial cell cultures (20 mL) were grown to mid-exponential phase (OD ~0.3) and fixed by the addition of sodium phosphate (pH 7.6) and formaldehyde to a final concentration of 10 mM and 1%, respectively. When treated with rifampicin, cells were incubated with 25 μg mL^{-1} rifampicin for 30 minutes prior to being fixed. Fixed cells were incubated at room temperature (RT) for 10 minutes and quenched with 0.1 M glycine for 5 min at RT followed by 15 min on ice. Cells were washed three times with 1X PBS (pH 7.4) and resuspended in 500 μL of TES buffer (10 mM Tris-HCl (pH 7.5), 1 mM EDTA, 100 mM NaCl) to which 1 μL of (35,000 U/μL) Ready-Lyse (Epicentre) was added. Following 15 min incubation at RT, 500 μL of ChIP buffer (16.7 mM Tris-HCl (pH 8.1), 167 mM NaCl, 1.1% Triton X-100, 1.2 mM EDTA) containing protease inhibitors (Roche cOmplete EDTA-free tablets) was added. After 10 min at 37 °C, the lysates were sonicated on ice and cell debris cleared by centrifugation. Supernatant protein concentration was measured by Bradford assay (Thermo Scientific) and 500 μg of proteins were diluted into 1 mL of ChIP buffer + 0.01% SDS. The diluted supernatants were pre-cleared for 1 hr at 4 °C on a rotator with 50 μL of Protein-A dynabeads (Life Technologies) pre-blocked overnight in ChIP buffer + 0.01% SDS and 100 μg BSA. Beads were pelleted and 90 μL of the supernatant was removed as input DNA and stored at -80 °C, the remaining pre-cleared supernatant was incubated rotating at 4 °C overnight with a specific antibody (Flag antibody 1:200 (Sigma Aldrich) or monoclonal RpoD antibody 1:166 (Neoclone, #WP004)). The immune complexes were captured for 2 hr at 4 °C with 50 μL of pre-blocked Protein-A dynabeads. Beads were then washed consecutively at 4 °C for 15 min with 1 mL of the following buffers: low salt wash buffer (0.1% SDS, 1% Triton X-100, 2 mM EDTA, 20 mM Tris-HCl (pH 8.1), 150 mM NaCl), high salt wash buffer (0.1% SDS, 1% Triton X-100, 2 mM EDTA, 20 mM Tris-HCl (pH

8.1), 500 mM NaCl), LiCl wash buffer (0.25 M LiCl, 1% NP-40, 1% deoxycholate, 1 mM EDTA, 10 mM Tris-HCl (pH 8.1) and twice with TE buffer (10 mM Tris-HCl (pH 8.1),1 mM EDTA). Complexes were then eluted twice from the beads with 250 µL of freshly prepared elution buffer (1% SDS, 0.1 M $NaHCO_3$). For reverse-crosslinking, 300 mM of NaCl and 2 µL of RNase A (0.5 mg / mL) (Qiagen) were added to the collective eluates which were incubated at 65 °C overnight. Samples were then incubated at 45 °C for 2 hr with 5 µL of Proteinase-K (NEB, 20 mg / ml) in the presence of 40 mM EDTA (pH 8.0) and 40 mM Tris-HCl (pH 6.8). DNA from the samples was then extracted twice with phenol:chloroform:isoamyl alcohol (25:24:1) and subsequently precipitated by adding sodium acetate (pH 5.2), 100 µg glycogen (Roche) and 1 volume of ice cold isopropanol, and stored at -20 °C overnight. DNA was pelleted and washed with 75% ethanol and resuspended in TE buffer (pH 8.0). Samples were analyzed by next-generation sequencing or qPCR.

Library generation and Illumina sequencing

Library generation and Illumina sequencing were performed at the MIT BioMicro Center. Libraries were generated on a Beckman-Colter Genomics SPRIworks system using 200-400 bp size selection and amplified 12-16 cycles. Up to 13 samples were multiplexed on one lane in a 40 nts single-read flow cell using the HiSeq2000 or 70 nts single-read flow cell using the MiSeq. For a summary of strains and conditions for which ChIP-Seq was performed, see Table S7. For ChIP-Seq data, see Table S8.

ChIP-Seq Analysis

Data processing: Reads were mapped to the *Caulobacter crescentus* NA1000 reference genome using BWA (Li and Durbin 2010). 750,000 uniquely mapping reads were taken for each sample. Read extension and pile-up was performed using the MACS software package 1.4.2 (Zhang et al. 2008) (with d=200 and keeping all tags at the same location) yielding 10 bp genomic bins containing the number of reads. The data were further process using custom scripts written in Python 2.7.3. The data were smoothed by convolution with a Gaussian (μ=0, σ=50bp, x=(-200 bp, +200 bp)). The data were then normalized in reads per million (rpm).

Peak-calling: As the control data presents a uniform background, (except for a slight bias due to the fact that ChIP was performed on a mixed population of cells undergoing replication, resulting

in a modest enrichment in DNA near the origin of replication), we used a sliding window looking for local maxima to call peaks. Local maxima were scored as peaks if they were 2.3-fold above the mean of the control sample, which corresponds to 5 standard deviations above the mean. Promoters were mapped from the peak summits identified from the RNAP rifampicin-treated ChIP sample, in which RNAP is trapped at promoters.

Normalization of ChIP-Seq data: In Fig. 1C, ChIP-Seq signals for GcrA, RNAP and σ^{70} were normalized such that the average of the 20 largest peaks at promoters (promoters were identified from RNAP signal in rifampicin-treated cells) for each ChIP experiment was 1.0. Active σ^{70} promoters were selected above a threshold of 0.1 (in normalized signal) and sorted based on σ^{70} signal. GcrA, RNAP and σ^{70} signals for selected promoters were plotted over 1 kb centered at the promoter if the signal for at least one of the proteins was > 0.2 normalized signal. In Figure 1D, ChIP-Seq signals were normalized as in Fig. 1C and a given promoter was classified as σ^{70}-, σ^{54}- or σ^{32}- dependent promoter based on the maximum of the normalized signals, with the condition that the normalized σ^{70} signal must be > 0.1 for a σ^{70} promoter and < 0.1 for a σ^{32} or σ^{54} promoter. Each promoter class was sorted based on the σ signal, and GcrA, RNAP and σ^{70}, σ^{54} and σ^{32} signals for selected promoters were plotted over a 1 kb interval, centered at the promoter if the signal for at least one protein was > 0.2.

Identification of GcrA sequence binding specificity

In Fig. 3B, 20 methylation sites were identified that had ChIP enrichment < 4 rpm for RNAP and > 7.0 rpm for GcrA. Methylation sites were excluded if they were in close proximity to other methylation sites or a promoter. A motif search was performed on these 20 sequences using MEME (Bailey et al. 2009). In Fig. 3C, the average ChIP enrichment for GcrA and σ^{70} for each of the 32 possible NGANTCN sequences was computed at non-promoter sequences (ChIP RNAP < 3 rpm) using data from rif-treated cells. In Fig. 3E, 25 promoters with the highest ChIP GcrA:σ^{70} ratios were isolated from a distribution computed from all σ^{70} promoters with σ^{70} signal > 6.0 rpm. In Fig. 3F, ChIP GcrA:σ^{70} ratios were computed at all transcription start sites mapped with σ^{70} signal > 6 rpm.

ChIP and Quantitative PCR analysis

In Fig. 2G, ChIP was performed as detailed above on strains ML2308, ML2312, ML2313, and ML2314 that had been depleted for 2 hours of untagged GcrA (cells were washed three times with PYE and released in PYE without vanillate) and then induced for two more hours by addition of 0.3% xylose to express a 3xFLAG tagged variant of GcrA or harboring an empty vector. For each sample, two ChIP reactions were performed for GcrA and σ^{70} using an anti-FLAG antibody and an anti-σ^{70} antibody, respectively. Quantitative PCR was performed with SYBR Green (Roche) on a Lightcycler 480 system (Roche). Each reaction contained 5 µL SYBR Green Master, 1 µL DNA (diluted 1:500 for pre-ChIP input DNA, and 1:10 for post-ChIP output DNA), 0.5 µL primer mix at 10 µM, and 3.5 µL nuclease-free water. Amplification of a region within the *ruvA* coding sequence was used as a control. Cycle threshold values were calculated using the Lightcycler 480 software and converted to DNA concentrations based on a standard curve generated from 3-fold dilutions of *Caulobacter* genomic DNA. Fold enrichment values were calculated as:

([OUTPUT($P_{of\ interest}$)]/[OUTPUT(*ruvA*)])/([INPUT($P_{of\ interest}$)]/[INPUT(*ruvA*)]).

The GcrA:σ^{70} enrichment ratio was then calculated and normalized to the GcrA:σ^{70} enrichment ratio calculated for the empty vector sample. Error bars were generated from two biological replicates and represent the standard deviation.

Protein expression and purification

Caulobacter RNAP: The purification protocol for RNAP was adapted from (Anthony et al. 2000). 10 L of *Caulobacter* ML2315 expressing RpoC-His_{10} from the native *rpoC* locus were grown in PYE to an OD_{600} of 0.4-0.6 and harvested by centrifugation. Cell pellets were resuspended in 40 mL lysis buffer P (300 mM NaCl, 50 mM Na_2HPO_3/NaH_2PO_3 (pH 8.0), 3 mM 2-mercaptoethanol, 5% glycerol) supplemented with cOmplete EDTA-free protease inhibitor cocktail (Roche), 40 mg lysozyme (Thermo Scientific) and 400 U benzonase (Novagen) and lysed by sonication. Lysates were cleared by centrifugation at 17,000 *g* for 45 min and then bound to Ni-NTA agarose (Qiagen) for 1 hr at 4 °C on a rotator in batch format. The resin was then washed with 40 mL of lysis buffer P, followed by 40 mL of lysis buffer P + 60 mM imidazole. RNAP was eluted in 2.5 mL of lysis buffer P + 250 mM imidazole and buffer

exchanged into TGED + 150 mM NaCl (50 mM Tris–HCl (pH 8.0), 5% glycerol, 0.1 mM EDTA, 0.1 mM DTT) on a PD-10 column (GE Healthcare). A second purification step was performed on a size exclusion column (16/600 Superdex 200 GE Healthcare) equilibrated with TGED + 150 mM NaCl. Fractions containing RNAP verified by Coomassie staining were pooled and run on a Mono Q Ion-Exchange chromatography column (Mono Q 10/100 GE Healthcare) pre-equilibrated with TGED + 150 mM NaCl. RNAP was eluted with a linear gradient up to TGED + 0.5 M NaCl over 15 column volumes. This yielded two separate peaks corresponding to RNAP core and RNAP holoenzyme as confirmed by Western blotting with anti-His, RpoA, and RpoD antibodies. Fractions from each peak were pooled, concentrated, buffer exchanged on an Amicon 3K Centrifugal filter unit (Millipore) into storage buffer (50 mM Tris–HCl (pH 8.0), 150 mM NaCl, 50% glycerol, 3 mM 2-mercaptoethanol) and stored at -20 °C. Protein concentration was measured by Bradford assay (Thermo Scientific).

His_6-tagged proteins: For His_6-GcrA and His_6-CcrM, cells were grown to OD_{600} ~ 0.5 at 37 °C and induced with 0.3 mM IPTG for 4 hr at 30 °C. For His_6-RpoD, His_6-RpoN, and His_6-RpoH, cells were induced overnight at 18 °C. Cells were harvested by centrifugation and resuspended in 20 mL lysis buffer (20 mM Tris-HCl (pH 7.9), 0.5 M NaCl, 0.1% Triton X-100, 10% glycerol) per liter of culture supplemented with 20 mg of lysozyme, 1 mM PMSF and 200 U benzonase (Novagen). Cells were lysed by sonication and cell debris cleared by centrifugation for 45 min at 17,000 *g*. Cleared lysates were bound to Ni-NTA agarose resin (Qiagen) for 30 min in batch format at 4 °C. Resin was washed twice with wash buffer (20 mM Hepes-KOH (pH 8.0), 0.5 M NaCl, 0.1% Triton X-100, 10% glycerol, 20 mM Imidazole) and proteins were eluted in 2.5 mL of elution buffer (20 mM Hepes-KOH (pH 8.0), 0.5 M NaCl, 10% glycerol, 250 mM imidazole) and buffer exchanged on PD-10 columns (GE Healthcare) into storage buffer. Storage buffer for His_6-RpoD, His_6-RpoH, and His_6-RpoN was 10 mM HEPES-KOH (pH 8.0), 50 mM KCl, 10% glycerol, 1 mM DTT, 0.1 mM EDTA), for His_6-CcrM it was 50 mM HEPES (pH 7.5), 200 mM NaCl, 0.1 mM DTT, 10% glycerol, and for His_6-GcrA it was 50 mM Tris-HCl (pH 8.5), 200 mM NaCl, 5 % glycerol. His_6-GcrA was further purified on a size exclusion column (16/600 Superdex 75, GE Healthcare) pre-equilibrated with GcrA storage buffer. Fractions containing His_6-GcrA were verified by Coomassie staining, pooled, and concentrated on an Amicon 10K Centrifugal filter unit (Millipore). Proteins were stored at -80 °C.

GST-tagged proteins: GST-GcrA and GST proteins were induced and purified in a similar manner as His_6-tagged proteins except that lysates were bound to 500 µL glutathione sepharose 4B beads (GE Healthcare) for 1 hr. Proteins were eluted in elution buffer (50 mM Tris-HCl (pH 8.0), 10 mM reduced glutathione) and buffer exchanged into GcrA storage buffer.

Antibody production

Rabbit polyclonal antisera (Covance) were generated from purified His_6-GcrA from which the His_6 tag was removed by digestion with TEV protease.

Affinity Chromatography

100 µL of pre-washed glutathione sepharose 4B beads (GE Healthcare) in binding buffer (50 mM HEPES-KOH (pH 7.5), 100 mM KCl, 0.1 mM EDTA, 2.5 mM $MgCl_2$, 3 % glycerol, 0.1 % Triton X-100) were incubated with 1 mg of GST-tagged protein for 1 hr at 4 °C with rotation. Beads were washed twice with 1 mL of binding buffer and then cleared WT *Caulobacter* lysate (Fig. 2A) (from 100 mL of cells grown to OD_{600} ~ 0.3 and lysed by sonication in binding buffer supplemented with lysozyme, benzonase, and cOmplete protease inhibitor cocktail (Roche)) or 0.25 mg of purified bait protein (His_6-RpoD, His_6-RpoH, His_6-RpoN) (Fig. 2E) was added. After incubation at 4 °C for 1 hr, beads were transferred to a 1 mL Bio-Spin chromatography column (Bio-Rad) and washed with 5 column volumes of binding buffer. Proteins were eluted three times with 50 µL elution buffer (50 mM Tris-HCl (pH 8.0), 10 mM reduced glutathione). Eluates were pooled and analyzed by gel electrophoresis and coomassie staining or Western blotting.

Co-Immunoprecipitation

1.5 L of strain ML2299 or CB15N grown to OD_{600} ~ 0.5 were harvested by centrifugation and resuspended in lysis buffer (50 mM HEPES (pH 7.5), 150 mM KCl, 0.1 mM EDTA, 5 mM $MgCl_2$, 5% glycerol). Cells were lysed by sonication and lysates were cleared by centrifugation at 17,000 *g* for 45 min. Cleared lysates were then bound to 200 µL of pre-equilibrated anti-FLAG magnetic beads (Sigma-aldrich) for 2 hr at 4 °C with rotation. Beads were washed three times with binding buffer and immunoprecipitated proteins were eluted with 100 µL of TBS (50 mM Tris-HCl (pH 7.4), 150 mM NaCl) buffer containing 100 µg/mL of 3xFLAG peptide (Sigma-aldrich). Eluates were analyzed by Western blotting.

DNA probe generation and labeling

DNA probe construction: Primers for probe amplification are listed in Table S6. Probes for the promoters of *ftsZ*, *mipZ* and *cckA* were PCR amplified with primer pairs (FB-ftsz-F, FB-ftsZ-R), (FB-mipz-F, FB-mipz-R) and (FB-cckA-F, FB-cckA-R), respectively. Mutations in P_{mipZ} were introduced by SOE-PCR with primer pairs (FB-mipz-F, FB-mipZ-R-soe-mutants and FB-mipZ-G3TG6A-T0GG6T, FB-mipZ-R-soe-outside) for $P_{mipZ(LM)}$ and (FB-mipz-F, FB-mipZ-R-soe-mutants and FB-mipZ-A4TG1C, FB-mipZ-R-soe-outside) for $P_{mipZ(NM)}$. Final PCR products were sequence verified and DNA probes were PCR amplified using the same primers as for the P_{mipZ} probe. Mutants of $P_{cckA,}$ $P_{cckA(LM)}$ and $P_{cckA(NM),}$ were PCR with the same primers as for the P_{cckA} probe using ordered gblock (IDT) as templates. All probes were between 136 to 193 bp and centered at the promoter as defined from transcription start site mapping. Two to four PCR reactions were gel purified (Qiagen) and pooled.

Methylation and probe labeling: Probes were methylated for at least 4 hr in 100 µL in the presence of purified His_6-CcrM, as described previously (Albu et al. 2012). Methylation was verified by digestion with HinfI, which cuts unmethylated GANTC sites. To distinguish full-methylation from hemi-methylation we digested a methylated probe sensitive to ClaI in the un-methylated or hemi-methylated state but resistant if fully-methylated. No digestion was observed in the methylated state after ClaI incubation, indicating complete methylation. Methylation reactions were PCR purified (Qiagen) and resuspended in 30 µL. Probes were labeled with T4-polynucleotide kinase (NEB) in 10 µL reactions containing 7 µL DNA, 1 µL of radiolabeled γ-P^{32} ATP, 1 µL of T4-PNK, and 1 µL of T4-PNK buffer at 37 °C for 90 min. Probes were then PCR purified and stored at -20 °C.

Filter binding assays

Open complex assay: Kinetic assays were performed at 30 °C. Reaction mixes were made in which an individual time point reaction was 15 µL including 8 µL of *Caulobacter* RNAP holoenzyme diluted in transcription buffer (40 mM Tris-HCl, (pH 8.0), 100 mM NaCl, 10 mM $MgCl_2$, 1.4% Tween-20, 50 µg/mL BSA (Ambion), and 1 mM DTT) and 2 µL of GcrA diluted in GcrA storage buffer. This was incubated for 10 min at 30 °C prior to addition of 5 µL of labeled DNA (0.1-0.25 nM) diluted in (10 mM Tris-HCl, (pH 8.5)) and pre-incubated at 30 °C for 10 min. Aliquots (14 µL) were removed at the indicated times and challenged with 2 µL heparin (50

µg/mL final) for 20 seconds, bound to prewashed nitrocellulose filters (Millipore) and immediately washed with 4 x 1 mL of wash buffer (10 mM Tris-HCl (pH 8.0), 100 mM NaCl, 1 mM EDTA). Filters were then incubated in 4 mL of scintillation liquid (National Diagnostics) and counts were read on a scintillation counter Tri-Carb 2910 TR (Perkin Elmer).

Background counts were subtracted and the fraction of DNA retained on the filter was plotted versus time. 100% DNA retained on filter was determined from reactions containing saturating levels of GcrA (4uM) or RNAP (20nM) without heparin competition and filtered. Curves were fitted with a single exponential, and the association rate k_{obs} was corrected for fractional occupancy (Barker et al. 2001). Obtained k_{obs} were plotted versus RNAP concentration and K_B and k_i were estimated by fitting the resulting curves to $k_{obs} = \frac{K_B * k_i * [RNAP]}{1 + K_B * [RNAP]}$ (Saecker et al. 2002). As P_{cckA} forms short-lived open complexes, P_{cckA} kinetics were performed in presence of 1 mM ATP to stabilize the open complex (ATP is the substrate for the first two nucleotides) enabling more accurate measurements and therefore the 2 first NTP binding steps make a slight contribution to k_i.

DNA binding assay: 2 µL of GcrA diluted in GcrA storage buffer and 8 µL of transcription buffer (40 mM Tris-HCl (pH 8.0), 100 mM NaCl, 10 mM $MgCl_2$, 1.4% Tween-20, 50 µg/mL BSA, and 1 mM DTT) were pre-incubated at 30 °C for 10 min. 5 µL of labeled DNA (1 nM) diluted in (10 mM Tris-HCl, (pH 8.5)) and pre-incubated at 30 °C for 10 min was added. Reactions were incubated at 30 °C for 5 min, bound to prewashed filters (Millipore) and immediately washed with 4 x 1 mL of wash buffer (10 mM Tris-HCl (pH 8.0), 100 mM NaCl, 1 mM EDTA). Counts were read similarly as in the open complex assays. K_d curves were fitted using the Prism software using one site specific binding with Hill slope and curves were normalized to the predicted B_{max}.

In vitro Transcription Assays

All assays were performed at 30 °C. In single-round *in vitro* transcription (Fig. 5D), reaction mixes were made in which an individual time point reaction was 15 µL including 8 µL of *Caulobacter* RNAP holoenzyme diluted in transcription buffer (40 mM Tris-HCl, (pH 8.0), 100 mM NaCl, 10 mM $MgCl_2$, 1.4% Tween-20, 50 µg/mL BSA (Ambion), and 1 mM DTT) and 2 µL of GcrA diluted in GcrA storage buffer. This was incubated for 10 min at 30 °C. 5 µL of

DNA (0.1-0.25 nM) diluted in (10 mM Tris-HCl, (pH 8.5)) and pre-incubated at 30 °C for 10 min was added. Aliquots (14 µL) were removed at indicated times and added to 2 µL of transcription start mix (heparin (50 µg/mL final), GTP (200 µM final), CTP (200 µM final), ATP (200 µM final), UTP (10 µM final), [α-^{32}P]UTP (2 µCi), 20 U SUPERase In RNase inhibitor (Life Technologies)) for 20 min. Reactions were stopped by addition of an equal volume of stop buffer Novex TBE-Urea (Life Technologies), electrophoresed on 10% TBE-Urea polyacrylamide gels (Life Technologies) and dried gels were visualized by phosphorimaging. Experiments were performed in duplicates, one representative gel is shown.

In multiple-round *in vitro* transcription (Fig 5B, 5E, S5A), reactions containing 8 µL of *Caulobacter* RNAP holoenzyme diluted in transcription buffer (40 mM Tris-HCl, (pH 8.0), 100 mM NaCl, 10 mM $MgCl_2$, 1.4% Tween-20, 50 µg/mL BSA (Ambion), and 1 mM DTT) and 2 µL of GcrA diluted in GcrA storage buffer and 2µL of transcription start mix (GTP (200 µM final), CTP (200 µM final), ATP (200 µM final), UTP (10 µM final), [α-^{32}P]UTP (2 µCi), 20 U SUPERase In RNase inhibitor (Life Technologies)) were preincubated 30 °C for 10 min. 5 µL of DNA (0.25-0.5 nM) in 10 mM Tris-HCl, (pH 8.5) was then added to each reaction and reactions were stopped after 15 min by addition of an equal volume of stop buffer Novex TBE-Urea (Life Technologies), electrophoresed on 10% or 15% TBE-Urea polyacrylamide gels (Life Technologies) and dried gels were visualized by phosphorimaging. Quantifications were performed using ImageJ. Experiments were performed in duplicates, one representative gel is shown.

DNA Microarray Analysis

Synchronies of CB15N or ML2302 were performed on 200 mL of exponential phase cultures using Percoll (GE Healthcare) density gradient centrifugation. To pre-deplete for *gcrA*, ML2302 cells were washed three times in PYE and resuspended in PYE without vanillate for 30 min prior to synchrony. After synchrony, cells were resuspended in PYE and RNA collected at the appropriate cell-cycle time-point. RNA was extracted using the RNeasy mini kit (Qiagen). The generation of cDNA and hybridization to custom Agilent arrays was performed as described previously (Gora et al. 2010). To eliminate defective probes from the array we removed outlier probes that had values more than 5 standard deviations away from the mean of the other probes for that gene. 10% of the mean was used as a lower bound for the standard deviation. In the case

of a defective probe it was excluded for all arrays. Array values for all genes are given in Table 1.

Transcription start site mapping and open reading frame matching

Transcription start sites (TSS) were mapped using genome-wide 5' mRNA data (Schrader et al. 2014). Briefly, a sliding window was used to find local increase (step function) on the forward or reverse strands of the 5' mRNA data on either side (100 bp) of a promoter identified from the rif-treated RNAP ChIP peaks. The highest local increase was selected if above a certain threshold (count=8). The transcription start site was then matched to the nearest open reading frame on the same strand (up to 400 bp upstream and 150 bp downstream of the annotated open reading frame start). This process was hand-curated at the promoters of genes that are down-regulated in GcrA-depleted cells for which a promoter was not identified. The list of all TSS used for analysis related to Fig. 5 is listed in Table S2.

Defining the GcrA regulon

The GcrA regulon was defined based on genes fulfilling three criteria: (i) at least 1.75-fold lower expression levels in GcrA-depleted cells at 30 or 45 min post-synchrony compared to wild-type. However, genes whose down-regulation at 60 min was 1.25-fold greater than the down-regulation at 30 or 45 min post-synchrony were excluded because GcrA is maximally abundant at 30 and 45 min post-synchrony (Fig. 5A) and GcrA targets were expected to be maximally affected at the 30 and 45 min time points; (ii) a GcrA:σ^{70} ChIP enrichment ratio from rif-treated cells > $2^{\wedge -0.5}$ at the gene's promoter; (iii) a promoter-proximal GANTC site (within 40 base pairs of the TSS). We used the rifampicin-treated ChIP data rather than the non-rif treated data to compute the GcrA:σ^{70} ChIP enrichment ratio used to identify the GcrA regulon for two reasons: (i) More promoters have σ^{70} signal in rif-treated cells which allowed us to compute the ratio at more promoters, (promoters were identified as having a peak in the RNAP rif-treated ChIP (see above, transcription start site mapping and open reading frame matching)). (ii) The rif-treated data allowed the capture of more subtle effects as there were more promoters with a high GcrA:σ^{70} ChIP enrichment ratio in the rif-treated sample compared to the non-rif treated sample. Additionally, the promoters that were above the high ratio threshold only in the rif-treated but not in the non-rif treated showed a distribution of changes in gene expression in GcrA-depleted cells different than promoters with low GcrA:σ^{70} ChIP ratio whereas promoters that were above

the high ratio threshold only in the non-rif treated sample did not show a difference. This indicates that the rif-treated sample contains more information and would lead to fewer false negatives. The GcrA regulon is summarized in Table S3.

Cell-cycle patterns of the GcrA regulon

Cell-cycle expression patterns of genes in the GcrA regulon was taken from RNA-Seq data previously published (Fang et al. 2013). For each gene i, each RNA-Seq count value $x_{i,j}$ at time point j was normalized as: $log_2(x_{i,j}) - \frac{\sum_j^n log_2(x_{i,j})}{n}$.

Promoters activated at the swarmer-to-stalk transition (Fig. S5B) were identified using two criteria on the normalized data (Fang et al. 2013) (see normalization above): (i) a two-fold positive change at the swarmer-to-stalk transition (time point 0 and 1), (ii) a normalized swarmer time point < 0.0.

Bacterial two-hybrid assay

Bacterial two-hybrid assays were performed as previously described (Aakre et al. 2013).

Immunoblotting

Immunoblotting was performed as described previously (Jonas et al. 2013) with the following modifications: 10% or 12% Tris-HCl gels were used (Bio-Rad) and gels were imaged with a Typhoon scanner (GE Healthcare) or a FluorChem M Imager (ProteinSimple). Antibodies were used at the following concentrations: anti-RpoA (Neoclone #W0003, 1:7500), anti-RpoD (Neoclone #W0004, 1:3000), anti-GcrA (1:5000), anti-Venus (MA1-952 Life Technologies, 1:1000), anti-FLAG (Sigma-Aldrich, 1:5000).

Microscopy

Phase contrast images and time-lapse movies were taken on a Zeiss Observer Z1 microscope using a 100x/1.4 oil immersion objective and an LED-based Colibri illumination system using software Metamorph (Universal Imaging, PA). For phase contrast images, cells were fixed with 0.5% paraformaldehyde, pelleted, and resuspended in PBS. Fixed cells were spotted onto PYE 1.5% agarose pads and imaged. Cells examined were in mid-exponential phase.

For time-lapse microscopy of strains ML2317-ML2320, cells induced with IPTG for 3 hours were placed on a 1.5% low-melting agarose pad made with PYE supplemented with IPTG and imaged in a glass-bottomed petri dish wrapped with Parafilm to prevent desiccation. To pre-deplete GcrA (ML2318, ML2320), cells were washed 3 times in PYE to remove the inducer vanillate, resuspended in PYE + IPTG and pre-depleted for 30 minutes prior to placing on the agarose pad. Pictures were taken every 8 minutes, and temperature was maintained at 30 °C using the Zeiss Temp Module S1 and Heating Insert P S1. Automatic focusing was performed using the Zeiss Definite Focus module. To perform cell segmentation and tracking, images were processed using MicrobeTracker (Sliusarenko et al. 2011). For wild-type cells, cell division events were scored using MicrobeTracker algorithm 4 with the modified parameters: areaMax = 950, splitThreshold = 0.5. For GcrA-depleted cells, algorithm 4 was used and division events were hand-curated. Origin of replication foci were detected using spotFinderZ and hand-curated using spotFinderM (Sliusarenko et al. 2011). The time between the initiation of replication to the next replication initiation (replication to replication time) was scored as the number of frames in between two replication events in a stalked cell lineage multiplied by 8 minutes (time between frames). An initiation of replication event was defined as the appearance of a second fluorescent focus indicating that the *tetO* array at the origin had been replicated. The time of replication to division was scored as the number of frames between the appearance of a second focus and the frame of cell division multiplied by 8 minutes. 110, 76, 59, 50 inter-replication events were counted for wt (ML2317), GcrA-depleted (ML2318), *pstS::Tn*^{5} (Ml2319), *pstS::Tn*^{5} GcrA-depleted (ML2320), respectively. 149, 71, 94, 70 replication to division events were counted for wt (ML2317), GcrA-depleted (ML2318), *pstS::Tn*^{5} (Ml2319), *pstS::Tn*^{5} GcrA-depleted (ML2320), respectively.

Flow Cytometry

Flow cytometry was performed as described previously (Aakre et al. 2013).

Suppressor screen

To screen for suppressors of *gcrA*, a *gcrA* depletion strain (ML2305) was transposon mutagenized using the EZ-Tn5 kit (Epicentre) and plated onto PYE medium containing kanamycin (to select for transposon integration). Colonies that grew after 2-4 days were isolated for genomic DNA extraction. To map transposon insertion sites, genomic DNA from putative

suppressor strains was digested, self-ligated, and transformed into *pir*-116 *E. coli*. Plasmids were prepped from the resulting transformants and sequenced using the Ez-Tn5 FP-1 forward primer.

Supplemental References

Aakre CD, Phung TN, Huang D, Laub MT. 2013. A bacterial toxin inhibits DNA replication elongation through a direct interaction with the β sliding clamp. *Mol Cell* **52**: 617–628.

Albu RF, Jurkowski TP, Jeltsch A. 2012. The Caulobacter crescentus DNA-(adenine-N6)-methyltransferase CcrM methylates DNA in a distributive manner. *Nucleic Acids Res* **40**: 1708–1716.

Anthony LC, Artsimovitch I, Svetlov V, Landick R, Burgess RR. 2000. Rapid purification of His(6)-tagged Bacillus subtilis core RNA polymerase. *Protein Expr Purif* **19**: 350–354.

Bae B, Davis E, Brown D, Campbell EA, Wigneshweraraj S, Darst SA. 2013. Phage T7 Gp2 inhibition of Escherichia coli RNA polymerase involves misappropriation of σ70 domain 1.1. *Proc Natl Acad Sci U S A* **110**: 19772–19777.

Bailey TL, Boden M, Buske FA, Frith M, Grant CE, Clementi L, Ren J, Li WW, Noble WS. 2009. MEME SUITE: tools for motif discovery and searching. *Nucleic Acids Res* **37**: W202–208.

Barker MM, Gaal T, Josaitis CA, Gourse RL. 2001. Mechanism of regulation of transcription initiation by ppGpp. I. Effects of ppGpp on transcription initiation in vivo and in vitro. *J Mol Biol* **305**: 673–688.

Ely B. 1991. Genetics of Caulobacter crescentus. *Methods Enzymol* **204**: 372–384.

Evinger M, Agabian N. 1977. Envelope-associated nucleoid from Caulobacter crescentus stalked and swarmer cells. *J Bacteriol* **132**: 294–301.

Fang G, Passalacqua KD, Hocking J, Llopis PM, Gerstein M, Bergman NH, Jacobs-Wagner C. 2013. Transcriptomic and phylogenetic analysis of a bacterial cell cycle reveals strong associations between gene co-expression and evolution. *BMC Genomics* **14**: 450.

Gonin M, Quardokus EM, O'Donnol D, Maddock J, Brun YV. Regulation of Stalk Elongation by Phosphate inCaulobacter crescentus. http://jb.asm.org (Accessed December 14, 2014).

Gora KG, Tsokos CG, Chen YE, Srinivasan BS, Perchuk BS, Laub MT. 2010. A cell-type-specific protein-protein interaction modulates transcriptional activity of a master regulator in Caulobacter crescentus. *Mol Cell* **39**: 455–467.

Holtzendorff J, Hung D, Brende P, Reisenauer A, Viollier PH, McAdams HH, Shapiro L. 2004. Oscillating global regulators control the genetic circuit driving a bacterial cell cycle. *Science* **304**: 983–987.

Jonas K, Liu J, Chien P, Laub MT. 2013. Proteotoxic stress induces a cell-cycle arrest by stimulating Lon to degrade the replication initiator DnaA. *Cell* **154**: 623–636.

Karimova G, Pidoux J, Ullmann A, Ladant D. 1998. A bacterial two-hybrid system based on a reconstituted signal transduction pathway. *Proc Natl Acad Sci U S A* **95**: 5752–5756.

Li H, Durbin R. 2010. Fast and accurate long-read alignment with Burrows-Wheeler transform. *Bioinforma Oxf Engl* **26**: 589–595.

Saecker RM, Tsodikov OV, McQuade KL, Schlax PE, Capp MW, Record MT. 2002. Kinetic studies and structural models of the association of E. coli sigma(70) RNA polymerase with the lambdaP(R) promoter: large scale conformational changes in forming the kinetically significant intermediates. *J Mol Biol* **319**: 649–671.

Schrader JM, Zhou B, Li G-W, Lasker K, Childers WS, Williams B, Long T, Crosson S, McAdams HH, Weissman JS, et al. 2014. The coding and noncoding architecture of the Caulobacter crescentus genome. *PLoS Genet* **10**: e1004463.

Skerker JM, Prasol MS, Perchuk BS, Biondi EG, Laub MT. 2005. Two-component signal transduction pathways regulating growth and cell cycle progression in a bacterium: a system-level analysis. *PLoS Biol* **3**: e334.

Sliusarenko O, Heinritz J, Emonet T, Jacobs-Wagner C. 2011. High-throughput, subpixel precision analysis of bacterial morphogenesis and intracellular spatio-temporal dynamics. *Mol Microbiol* **80**: 612–627.

Thanbichler M, Iniesta AA, Shapiro L. 2007. A comprehensive set of plasmids for vanillate- and xylose-inducible gene expression in Caulobacter crescentus. *Nucleic Acids Res* **35**: e137.

Zhang Y, Liu T, Meyer CA, Eeckhoute J, Johnson DS, Bernstein BE, Nusbaum C, Myers RM, Brown M, Li W, et al. 2008. Model-based analysis of ChIP-Seq (MACS). *Genome Biol* **9**: R137.

Table S4: Strains

Name	Genotype	Source
***C. crescentus* strains**		
CB15N	Synchronizable wild-type CB15	(Evinger and Agabian 1977)
LS3707	*gcrA(spec^R)*; P$_{xyl}$-*gcrA(kan^R)*	(Holtzendorff et al. 2004)
ML2296	Δ*gcrA(tet^R)*; P$_{xyl}$-*gcrA(kan^R)*	This study
ML2297	Δ*gcrA(tet^R)*; P$_{xyl}$-*gcrA-3xFLAG(kan^R)*	This study
ML2298	*gcrA::gcrA-3xFLAG(kan^R)*	This study
ML2299	*rpoC::rpoC-3xFLAG(kan^R)*	This study
ML2300	*rpoH::rpoH-3xFLAG(kan^R)*	This study
ML2301	*rpoN::rpoN-3xFLAG(kan^R)*	This study
ML2302	Δ*gcrA(tet^R)*; P$_{van}$-*gcrA(kan^R)*	This study
ML2303	Δ*spoT*	Lab strain collection
ML2304	Δ*spoT ΔgcrA(spec^R)*; P$_{van}$-*gcrA(kan^R)*; pCT133-P$_{lacI}$-*lacI*-P$_{lac}$-*spoT(H67A)*	This study
ML2305	Δ*gcrA(spec^R)*; P$_{van}$-*gcrA(gent^R)*	This study
ML2306	ML2305 pMT375-*ftsN*	This study
ML2307	ML2305 pMT375-*ftsZ*	This study
ML2308	ML2305 pMT375	This study
ML2309	ML2305 pMT375-*gcrA*	This study
ML2312	ML2305 pMT375-*gcrA-3xFLAG*	This study
ML2313	ML2305 pMT375-*gcrA$_{1-107}$-3xFLAG*	This study
ML2314	ML2305 pMT375-*gcrA$_{51-173}$-3xFLAG*	This study
ML2315	*rpoC::rpoC-HIS$_{10}$ (kan^R)*	This study
YB767	*pstS::Tn^5*	(Gonin et al.)
ML2316	Δ*gcrA(spec^R)*; P$_{van}$-*gcrA(gent^R)*; *pstS::Tn^5*	This study
ML1678	*Cori::tetO(gent^R); (LacI-CFP and TetR-YFP)(spec ^{R}); integrated at xylX locus*	Lab strain collection
ML2317	*Cori::tetO(gent^R); hfaA::*P$_{lacI}$-*lacI*-P$_{lac}$-*tetR-mCerulean*	Lab strain collection
ML2318	*Cori::tetO(gent^R); hfaA::*P$_{lacI}$-*lacI*-P$_{lac}$-*tetR-mCerulean;* P$_{van}$-*gcrA(rif^R); ΔgcrA(tet^R)*	This study
ML2319	*Cori::tetO(gent^R); hfaA::*P$_{lacI}$-*lacI*-P$_{lac}$-*tetR-mCerulean; pstS::Tn^5*	This study
ML2320	*Cori::tetO(gent^R); hfaA::*P$_{lacI}$-*lacI*-P$_{lac}$-*tetR-mCerulean;* P$_{van}$-*gcrA(rif^R); ΔgcrA(tet^R); pstS::Tn^5*	This study

ML2475	*CCNA_02236□P$_{mipZ}$-venus (kan^R)*	This study
ML2476	*CCNA_02236□P$_{mipZ}$(LM)-venus (kan^R)*	This study
ML2477	*CCNA_02236□P$_{mipZ}$(NM)-venus (kan^R)*	This study
E. coli strains		
DH5α	General cloning strain	Invitrogen
TOP10	General cloning strain	Invitrogen
BL21DE3 pLysS	Strain for protein expression and purification	Novagen
BTH101	Strain for bacterial two-hybrid assay	Euromedex
ML2321	BTH101 pUT18C pKT25	This study
ML2322	BTH101 pUT18C-*gcrA* pKT25	This study
ML2323	BTH101 pUT18C-*gcrA* pKT25-*rpoA*	This study
ML2324	BTH101 pUT18C-*gcrA* pKT25-*rpoB*	This study
ML2325	BTH101 pUT18C-*gcrA* pKT25-*rpoC*	This study
ML2326	BTH101 pUT18C-*gcrA* pKT25-*rpoZ*	This study
ML2327	BTH101 pUT18C-*gcrA* pKT25-*rpoD*	This study
ML2328	BTH101 pUT18C pKT25-*rpoA*	This study
ML2329	BTH101 pUT18C pKT25-*rpoB*	This study
ML2330	BTH101 pUT18C pKT25-*rpoC*	This study
ML2331	BTH101 pUT18C pKT25-*rpoZ*	This study
ML2332	BTH101 pUT18C pKT25-*rpoD*	This study
ML2333	BTH101 pUT18 pKNT25	This study
ML2334	BTH101 pUT18-*gcrA* pKNT25-*rpoD*	This study
ML2335	BTH101 pUT18-*gcrA* pKNT25-*rpoH*	This study
ML2336	BTH101 pUT18-*gcrA* pKNT25-*rpoN*	This study
ML2337	BTH101 pUT18-*gcrA* pKNT25	This study
ML2338	BTH101 pUT18 pKNT25-*rpoD*	This study
ML2339	BTH101 pUT18 pKNT25-*rpoH*	This study
ML2340	BTH101 pUT18 pKNT25-*rpoN*	This study
ML2341	BTH101 pUT18-*gcrA* pKNT25-*rpoD*$_{1-574}$	This study
ML2342	BTH101 pUT18-*gcrA* pKNT25-*rpoD*$_{1-484}$	This study
ML2343	BTH101 pUT18-*gcrA* pKNT25-*rpoD*$_{107-484}$	This study
ML2344	BTH101 pUT18 pKNT25-*rpoD*$_{1-574}$	This study
ML2345	BTH101 pUT18 pKNT25-*rpoD*$_{1-484}$	This study
ML2346	BTH101 pUT18 pKNT25-*rpoD*$_{107-484}$	This study
ML2347	BTH101 pUT18C-*gcrA*$_{1-50}$ pKT25-*rpoD*	This study

ML2348	BTH101 pUT18C-*gcrA*$_{108-173}$ pKT25-*rpoD*	This study
ML2349	BTH101 pUT18C-*gcrA*$_{1-50}$ pKT25	This study
ML2350	BTH101 pUT18C-*gcrA*$_{108-173}$ pKT25	This study
ML2351	BTH101 pUT18-*gcrA* pKNT25-*CCNA_00393*	This study
ML2352	BTH101 pUT18-*gcrA* pKNT25-*CCNA_00596*	This study
ML2353	BTH101 pUT18-*gcrA* pKNT25-*CCNA_00685*	This study
ML2354	BTH101 pUT18-*gcrA* pKNT25-*CCNA_01032*	This study
ML2355	BTH101 pUT18-*gcrA* pKNT25-*CCNA_01187*	This study
ML2356	BTH101 pUT18-*gcrA* pKNT25-*CCNA_01390*	This study
ML2357	BTH101 pUT18-*gcrA* pKNT25-*CCNA_01718*	This study
ML2358	BTH101 pUT18-*gcrA* pKNT25-*CCNA_01721*	This study
ML2359	BTH101 pUT18-*gcrA* pKNT25-*CCNA_02790*	This study
ML2360	BTH101 pUT18-*gcrA* pKNT25-*CCNA_02837*	This study
ML2361	BTH101 pUT18-*gcrA* pKNT25-*CCNA_02977*	This study
ML2362	BTH101 pUT18-*gcrA* pKNT25-*CCNA_03273*	This study
ML2363	BTH101 pUT18-*gcrA* pKNT25-*CCNA_03362*	This study
ML2364	BTH101 pUT18-*gcrA* pKNT25-*CCNA_03375*	This study
ML2365	BTH101 pUT18-*gcrA* pKNT25-*CCNA_03419*	This study
ML2366	BTH101 pUT18-*gcrA* pKNT25-*CCNA_03589*	This study
ML2563	BTH101 pUT18 pKNT25-*CCNA_00393*	This study
ML2564	BTH101 pUT18 pKNT25-*CCNA_00596*	This study
ML2565	BTH101 pUT18 pKNT25-*CCNA_00685*	This study
ML2566	BTH101 pUT18 pKNT25-*CCNA_01032*	This study
ML2567	BTH101 pUT18 pKNT25-*CCNA_01187*	This study
ML2568	BTH101 pUT18 pKNT25-*CCNA_01390*	This study
ML2569	BTH101 pUT18 pKNT25-*CCNA_01718*	This study
ML2570	BTH101 pUT18 pKNT25-*CCNA_01721*	This study
ML2571	BTH101 pUT18 pKNT25-*CCNA_02790*	This study
ML2572	BTH101 pUT18 pKNT25-*CCNA_02837*	This study
ML2573	BTH101 pUT18 pKNT25-*CCNA_02977*	This study
ML2574	BTH101 pUT18 pKNT25-*CCNA_03273*	This study
ML2575	BTH101 pUT18 pKNT25-*CCNA_03362*	This study
ML2576	BTH101 pUT18 pKNT25-*CCNA_03375*	This study
ML2577	BTH101 pUT18 pKNT25-*CCNA_03419*	This study
ML2578	BTH101 pUT18 pKNT25-*CCNA_03589*	This study
ML2367	BTH101 pUT18-*gcrA* pKNT25-*rpoD-*σ_2*-chimera1(Cc*$_{107-}$	This study

	$_{159}$-Ec$_{139-349}$-Cc$_{390-484}$)	
ML2368	BTH101 pUT18-*gcrA* pKNT25-*rpoD-σ$_2$-chimera2(Ec$_{89-138}$-Cc$_{160-389}$-Ec$_{350-444}$)*	This study
ML2369	BTH101 pUT18-*gcrA* pKNT25-*rpoD-σ$_2$-Ecoli$_{89-444}$*	This study
ML2579	BTH101 pUT18 pKNT25-*rpoD-σ$_2$-chimera1(Cc$_{107-159}$-Ec$_{139-349}$-Cc$_{390-484}$)*	This study
ML2580	BTH101 pUT18 pKNT25-*rpoD-σ$_2$-chimera2(Ec$_{89-138}$-Cc$_{160-389}$-Ec$_{350-444}$)*	This study
ML2581	BTH101 pUT18 pKNT25-*rpoD-σ$_2$-Ecoli$_{89-444}$*	This study
ML2370	BL21DE3 pLysS pGEX-4T2	This study
ML2371	BL21DE3 pLysS pGEX-4T2-*gcrA*	This study
ML2372	BL21DE3 pLysS pET28b-HIS$_6$-*gcrA*	This study
ML2373	BL21DE3 pLysS pET28b-HIS$_6$-*rpoD*	This study
ML2374	BL21DE3 pLysS pET28b-HIS$_6$-*rpoH*	This study
ML2375	BL21DE3 pLysS pET28b-HIS$_6$-*rpoN*	This study
ML2378	BL21DE3 pLysS pET28b-HIS$_6$-*ccrM*	This study

Table S5: Plasmids

Plasmids	Description/purpose	Source
pENTR/D-TOPO	Entry vector for Gateway cloning (kan^R)	Invitrogen
pNPTS138	Integration vector (kan^R) with *sacB* counterselection	Lab collection
pNPTS-spec-DEST	pNPTS138 derivative modified with $spec^r$ cassette	(Gora et al. 2010)
pMT375 (pRXMCS-5)	Low-copy plasmid for xylose inducible expression of genes (tet^R)	(Thanbichler et al. 2007)
pMT585 (pXGFPC-2)	Vector for integration at P_{xyl} (kan^R)	(Thanbichler et al. 2007)
pMT552 (pVGPFC-2)	Vector for integration at P_{van}(kan^R)	(Thanbichler et al. 2007)
pMT644 (pVGFPC-4)	Vector for integration at P_{van}($gent^R$)	(Thanbichler et al. 2007)
pMT561(pVGFPC-3)	Vector for integration at P_{van}(rif^R)	(Thanbichler et al. 2007)
pCT133	Low-copy destination vector (tet^R)	Lab collection
pKO3	Template for tet cassette amplification	Lab collection
pENTR-spec-UP-tet-DW(*gcrA*)	pENTR containing sequence for *tet*-marked in frame deletion of *gcrA*	This study
pNPTS-spec-UP-tet-DW(*gcrA*)	*tet*-marked in frame deletion of *gcrA*	This study
pMT585-*gcrA*	Integration of P_{xyl}-*gcrA* at the xylose locus (kan^R)	This study
pMT585-*gcrA-3xFLAG*	Integration of P_{xyl}-*gcrA-3xFLAG* at the xylose locus (kan^R)	This study
pNPTS138-*gcrA-3xFLAG*	Single integration of *gcrA-3xFLAG* at *gcrA*	This study
pNPTS138-*rpoC-3xFLAG*	Single integration of *rpoC-3xFLAG* at *rpoC*	This study
pNPTS138-*rpoH-3xFLAG*	Single integration of *rpoH-3xFLAG* at *rpoH*	This study
pNPTS138-*rpoN-3xFLAG*	Single integration of *rpoN-3xFLAG* at *rpoN*	This study
pNPTS138-*rpoC-HIS*$_{10}$	Single integration of *rpoC-HIS*$_{10}$ at *rpoC*	This study
pNPTS138-P_{mipZ}-*venus*	Integration of P_{mipZ}-*venus* at the CCNA_02236 locus	This study
pNPTS138-P_{mipZ}*(LM)-venus*	Integration of P_{mipZ}*(LM)-venus* at the CCNA_02236 locus	This study
pNPTS138-P_{mipZ}*(NM)-venus*	Integration of P_{mipZ}*(NM)-venus* at the CCNA_02236 locus	This study
pMT552-*gcrA*	Integration of P_{van}-*gcrA* at the van locus (kan^R)	This study
pNPTS-Δ*spoT*	Markerless deletion of *spoT*	Lab plasmid collection
pCT133-P_{lacI}-*lacI*-P_{lac}-*spoT(H67A)*	Expression of hydrolase-defective mutant of *spoT*	Lab plasmid collection
pNPTS138-hfaAUP-P_{lacI}-*lacI*-P_{lac}-tetR-mCerulean-	Integration of P_{lacI}-*lacI*-P_{lac}-tetR-mCerulean at the hfaA locus	Lab plasmid collection

hfaADW		
pMT561-*gcrA*	Integration of P_{van}-*gcrA* at the van locus (rif^R)	This study
pMT644-*gcrA*	Integration of P_{van}-*gcrA* at the van locus ($gent^R$)	This study
pMT375-*ftsN*	Xylose inducible expression of *ftsN*	This study
pMT375-*ftsZ*	Xylose inducible expression of *ftsz*	This study
pMT375-*gcrA*	Xylose inducible expression of *gcrA*	This study
pMT375-*gcrA-3xFLAG*	Xylose inducible expression of *gcrA-3xFLAG*	This study
pMT375-$gcrA_{1-107}$-*3xFLAG*	Xylose inducible expression of $gcrA_{1-107}$-*3xFLAG*	This study
pMT375-$gcrA_{51-173}$-*3xFLAG*	Xylose inducible expression of $gcrA_{51-173}$-*3xFLAG*	This study
pKT25	For generating genetic fusions of proteins to C-terminus of T25	(Karimova et al. 1998)
pKNT25	For generating genetic fusions of proteins to N-terminus of T25	(Karimova et al. 1998)
pUT18	For generating genetic fusions of proteins to N-terminus of T18	(Karimova et al. 1998)
pUT18C	For generating genetic fusions of proteins to C-terminus of T18	(Karimova et al. 1998)
pUT18C-*gcrA*	T18-GcrA	This study
pUT18-*gcrA*	GcrA-T18	This study
pUT18C-$gcrA_{1-50}$	T18-$GcrA_{1-50}$	This study
pUT18C-$gcrA_{108-173}$	T18-$GcrA_{108-173}$	This study
pKT25-*rpoA*	T25-RpoA	This study
pKT25-*rpoB*	T25-RpoB	This study
pKT25-*rpoC*	T25-RpoC	This study
pKT25-*rpoZ*	T25-RpoZ	This study
pKT25-*rpoD*	T25-RpoD	This study
pKNT25-*rpoD*	RpoD-T25	This study
pKNT25-*rpoH*	RpoH-T25	This study
pKNT25-*rpoN*	RpoN-T25	This study
pKNT25-$rpoD_{1-574}$	$RpoD_{1-574}$-T25	This study
pKNT25-$rpoD_{1-484}$	$RpoD_{1-484}$-T25	This study
pKNT25-$rpoD_{107-484}$	$RpoD_{107-484}$-T25	This study
pKNT25-*CCNA_00393*	CCNA_00393-T25	This study
pKNT25-*CCNA_00596*	CCNA_00596-T25	This study
pKNT25-*CCNA_00685*	CCNA_00685-T25	This study
pKNT25-*CCNA_01032*	CCNA_01032-T25	This study

pKNT25-*CCNA_01187*	CCNA_01187-T25	This study
pKNT25-*CCNA_01390*	CCNA_01390-T25	This study
pKNT25-*CCNA_01718*	CCNA_01718-T25	This study
pKNT25-*CCNA_01721*	CCNA_01721-T25	This study
pKNT25-*CCNA_02790*	CCNA_02790-T25	This study
pKNT25-*CCNA_02837*	CCNA_02837-T25	This study
pKNT25-*CCNA_02977*	CCNA_02977-T25	This study
pKNT25-*CCNA_03273*	CCNA_03273-T25	This study
pKNT25-*CCNA_03362*	CCNA_03362-T25	This study
pKNT25-*CCNA_03375*	CCNA_03375-T25	This study
pKNT25-*CCNA_03419*	CCNA_03419-T25	This study
pKNT25-*CCNA_03589*	CCNA_03589-T25	This study
pKNT25-*rpoD-σ_2-chimera1($Cc_{107-159}$-$Ec_{139-349}$-$Cc_{390-484}$)*	*rpoD-σ_2-chimera1($Cc_{107-159}$-$Ec_{139-349}$-$Cc_{390-484}$)*-T25	This study
pKNT25-*rpoD-σ_2-chimera2(Ec_{89-138}-$Cc_{160-389}$-$Ec_{350-444}$)*	*rpoD-σ_2-chimera2(Ec_{89-138}-$Cc_{160-389}$-$Ec_{350-444}$)*-T25	This study
pKNT25-*rpoD-σ_2-Ecoli$_{89-444}$*	*rpoD-σ_2-Ecoli$_{89-444}$*-T25	This study
pGEX-4T2	Expression vector with GST tag	Lab collection
pET28b	Expression vector with His_6 tag	Lab collection
pGEX-4T2-*gcrA*	Expression vector for purification of GST-GcrA	This study
pET28b-HIS_6-*gcrA*	Expression vector for purification of HIS_6-GcrA	This study
pET28b-HIS_6-*rpoD*	Expression vector for purification of HIS_6-RpoD	This study
pET28b-HIS_6-*rpoH*	Expression vector for purification of HIS_6-RpoH	This study
pET28b-HIS_6-*rpoN*	Expression vector for purification of HIS_6-RpoN	This study
pET28b-HIS_6-*ccrM*	Expression vector for purification of HIS_6-CcrM	This study

Table S6: Primers

Primer	Sequence (5'->3')
OL3_up_gcrA_F	CACCTCAGGAAGTCCGGCGTCAG
OL4_up_gcrA_R	CGATATCAAGCTTATCGATACCGGTCGGTCCAGCTCATTACCCGTCT
OL5_dw_gcrA_F	GGAACTTCTTGAATTCCTGCAGCTGGCCCGCTCGCTTCGCCGCTACATCTAAG
OL6_dw_gcrA_R	AGCGCGAGCCGGCCGGATAG
OL7_tet_F	CGGTATCGATAAGCTTGATATCG
OL8_tet_R	CTGCAGGAATTCAAGAAGTTCC
OL17_NdeI_gcrA_F	GATTCATATGAGCTGGACCGACGAACG
OL18_SacI_gcrA_R	GTAGGAGCTCTTAGATGTAGCGGCGAAGCG
OL69_del_gcrA_ver_F	CCGTAAGCCCGAAATAAAGCACCGCCCAGAGG
OL70_del_gcrA_ver_R	CGGTCGCGGATGCGGTGCAGGATGTCGCGGATC
GcrA-3xFLAGSOE-CTERM-R	CCGTCGTGGTCCTTGTAGTCGATGTAGCGGCGAAGCGAGCG
3xFLAG-F	GACTACAAGGACCACGACGGCG
3xFLAG-SACI-R	AGATACGAGCTCTTACTTGTCGTCGTCGTCCTTGTAGTCG
HindIII-GcrActerm3XFLAG_F	AGATAAGCTTCGGCCTTTCGGCCAGCCAGATC
rpoC-HindIII-Cterm-F	AGATACAAGCTTGGCAACCAGCCCGAGGCGGTCG
Rev-rpoC3Xflag	CCGTCGTGGTCCTTGTAGTCTTCGGCGTCCGAAAGCGCGATCTCG
RpoN-HindIII-3X-F	AGATAAGCTTATCTGCGGCGTCGACGACGAAGATC
rpoN-3X-R	CCGTCGTGGTCCTTGTAGTCGACCGCTTCCTTCATCAGCCGGC
rpoH-HindIII-3X-F	AGATAAGCTTATCCGCAAGCGGCCCACAAGATG
rpoH-3X-Flag-R	CCGTCGTGGTCCTTGTAGTCGGCGTCGACCATGTTCTTGGCGATC
Rev-3x flag EcorI	AGATACGAATTCTTACTTGTCGTCGTCGTCCTTGTAGTCG
rpoC-R1linker	TGGTGATGATGTGAACCGCCTGATCCGCCTTCGGCGTCCGAAAGCGCGATCTCG
rpoC-R2linker-10His	AGATGAATTCCTAGTGGTGATGATGGTGGTGATGGTGATGATGTGAACCGCCTGAT
FtsN-NdeI-F	AGATCATATGTCCGATCCGCACCGCGGG
FtsN-SacI-R	AGATGAGCTCTCACTTTACGAAGCAGGATTTGCCG
NdeI-FtsZ-F	AGATACCATATGGCTATTTCTCTTTCCGCGC
FtsZ-R-SacI	AGATGAGCTCTCAGTTGGCCAGGCGGCGCAG
NL-fuse3Xflag	CCGTCGTGGTCCTTGTAGTCCGAGCCGGGTTCTTCGTGACGG
GcrA-Cterm-151-F-NdeI	AGATCATATGCCCTCGCAACCGGCCCGTCCG

CAP133	AATTGAAGCCGGCTGGCGCCAAGCTTCGACGGCCTAGAGGGTGGACATC
CAP134	GTCCACCGTCTCAGACGACAACGCGCCCGATTC
CAP135	GCGTTGTCGTCTGAGACGGTGGACCGGACGCG
CAP136	GCGTCACGGCCGAAGCTAGCGAATTCATCCCGGTTGCCTCGGCATC
CAP173	GAGCGAACTGGAACTGGTCCG
CAP174	CACGCCGTCAGACTGCGTAAC
CAP66	GCGGCCGCCCCCTTCACCATGAATTCGCATGCATTTACGTTGACACCA
CAP391	CACAGACGACATAGCTGTTTCCTGTGTGAAATTGTTATCC
CAP392	CAGGAAACAGCTATGTCGTCTGTGGCCCCCGTC
CAP393	GCTCTAGAACTAGTGGATCCCCCGGGCTACCCCCGCGTCCGGTCCAC
CAP394	GCGATCCCTACTATGCTGCCCCGATCGAGGTGGCGG
CAP395	CCGCCACCTCGATCGGGGCAGCATAGTAGGGATCGC
CAP94	AATTGAAGCCGGCTGGCGCCAAGCTTACATCGGTCCAAGCTGGCC
CAP95	GTAAATGCATGCCCCAAGGTCTCGAAAAAATGGTTAAGCC
CAP96	CGAGACCTTGGGGCATGCATTTACGTTGACACCATCG
CAP137	TCTAGACATCATAGCTGTTTCCTGTGTGAAATTGTTATCCG
CAP138	CAGGAAACAGCTATGATGTCTAGATTAGATAAAAGTAAAGTGATTAACAGCG
CAP139	CTGTACAAGTAAGCTATCCCTCATGCTGTATCTTTTTGGC
CAP140	ATGAGGGATAGCTTACTTGTACAGCTCGTCCATGCCG
CAP99	GCGTCACGGCCGAAGCTAGCGAATTCTCATTTCGGAGTACCGCCCTTC
CAP60	GCCCTTGCTCACCAACTCGAGGATGTCAGACCCAC
CAP61	ATCCTCGAGTTGGTGAGCAAGGGCGAGGAG
F-GcrA-BamHI	GATTGGATCCATGAGCTGGACCGACGAACG
R-GcrA-SalI	GTAGGTCGACTTAGATGTAGCGGCGAAGCG
RpoD-pet28-NdeI-F	AGATCATATGTTGATGAGCAACAATTCCTCGGCC
rpoD-pet28-HindIII-R	AGATAAGCTTTTACGAGTCCAGGAAGCTGCGCAG
rpoH-pet28-NdeI-F	AGATCATATGAGTAAGATGGCCGTGAATTCTCTATCG
rpoH-pet28-HindIII-R	AGATAAGCTTCTAGGCGTCGACCATGTTCTTGG
rpoN-pet28-NdeI-F	AGATCATATGTTGGCGCTCAGCCACCGACTAG
rpoN-pet28-HindIII-R	AGATAAGCTTTCAGACCGCTTCCTTCATCAGCC
ccrm-NdeI-F	AGATCATATGAAGTTCGGGCCGGAAACC
ccrm-EcoRI-R	AGATGAATTCTCAGTTCATCCCCGCCCGCAC
GcrA-XbaI-F	AGATTCTAGAGATGAGCTGGACCGACGAACGG
GcrA-KpnI-stop-R	AGATGGTACCTTAGATGTAGCGGCGAAGCGAGC
GcrA-KpnI-R	AGATGGTACCCGGATGTAGCGGCGAAGCGAGCG
rpoA-XbaI-F	AGATTCTAGAGGTGATCGAAAGAAACTGGAACGAGCTG

rpoA-KpnI-stop-R	AGATGGTACCTTAGATCTGGTCTTCGAACTTCTTGGCC
rpoB-XbaI-F	AGATTCTAGAGATGGCGCAATCCTTCACCGGCAAG
rpoB-KpnI-stop-R	AGATGGTACCTCAGCTGTTCTCCAGCTCGACGTTC
rpoC-XbaI-F	AGATTCTAGAGATGAACCAGGAAGTCCTGAACATCTTCAATC
rpoC-KpnI-stop-R	AGATGGTACCCTATTCGGCGTCCGAAAGCGCG
omega-XbaI-F	AGATTCTAGAGATGGCCCGCGTCACCGTCGAAG
omega-KpnI-stopR	AGATGGTACCTCAGTACCGCTCCTCCTGACCAC
s70-XbaI-F	AGATTCTAGAGTTGATGAGCAACAATTCCTCGGCC
s70-KpnI-stop-R	AGATGGTACCTTACGAGTCCAGGAAGCTGCGCAG
s70-KpnI-R	AGATGGTACCCGCGAGTCCAGGAAGCTGCGCAGC
GcrA-1-150-stop-R	AGATGGTACCTTAAGCCGCGCGGCCCGACAGGCC
GcrA-322-end-F	AGATTCTAGAGGCCACCGTGCTGACCCTGGGCG
rpoH-F-b2h	AGATTCTAGAGATGAGTAAGATGGCCGTGAATTCTCTATCG
rpoH-R-b2h	AGATGGTACCCGGGCGTCGACCATGTTCTTGGCG
rpoN-F-b2h	AGATTCTAGAGTTGGCGCTCAGCCACCGACTAGAG
rpoN-R-b2h	AGATGGTACCCGGACCGCTTCCTTCATCAGCCGG
rpoDaa484-R	AGATGGTACCCGGGCGATCGAGCGGGTGATCGC
sig70-1-3-R	AGATGGTACCCGCGCGTCGATCGGCAGGATGGC
sig70nt319-F	AGATTCTAGAGGCGGCCTATGACCGCACCGACG
CCNA_00393-F-B2H	AGATTCTAGAGTTGAGCCCTCTCGATCAAACGGC
CCNA_00393-R-B2H	AGATGGTACCCGGTTGGCGCTTGCCATAAAGCTCC
B2H-00596-F	AGATTCTAGAGTTGCGGTATCCCGGGCCCAGG
B2H-00596-R	AGATGGTACCCGCAGCTCGAACCATCCATCCTCC
CCNA_00685-F	AGATTCTAGAGGTGGGCATGTATGCGACAGGAC
CCNA_00685-R	AGATGGTACCCGCGACGCGACTCCCGCCTCGCG
B2H-1032-F	AGATTCTAGAGTTGAGGGGAGCGTTGATGGCG
B2H-1032-R	AGATGGTACCCGCCGCTTCGCGTCGTGATCCCG
B2H-1187-F	AGATTCTAGAGATGAGCGATCTGGCGAGCCTG
B2H-1187-R	AGATGGTACCCGTGAGCGTCCCCCGCCTGCGCGAC
CCNA_01390-F-B2H	AGATTCTAGAGATGCTCTACGCCATTCTTTGCTACAACC
CCNA_01390-R-B2H	AGATGGTACCCGGACCCTGGTCGCCATCGTGTCC
B2H-1718-F	AGATTCTAGAGATGGACGCCGCGCTCGTCAG
B2H-1718-R	AGATGGTACCCGTCGAGATCCTCCCAGAACCGCC
B2H-1721-F	AGATTCTAGAGTTGATTTCAATGGGCATGGAACG
B2H-1721-R	AGATGGTACCCGGCCATGAGCTTCCCTCCTCGCG
B2H-2790-F	AGATTCTAGAGATGAGTAAAGTGAGACAATATCGTCGTGCG

B2H-2790-R	AGATGGTACCCGGCCCCGGATCATGTCGGCGC
B2H-2837-F	AGATTCTAGAGTTGGTCTCCGACGGGAACGATC
B2H-2837-R	AGATGGTACCCGCGCTTCGCCTCGCGTCAGATC
B2H-2977-F	AGATTCTAGAGATGGACCAGCAGACTCAGAAGAGCTTC
B2H-2977-R	AGATGGTACCCGTGCCGCCAGCCGTTCCAGATC
B2H-3273-F	AGATTCTAGAGGTGCGGACGGATGATCTGATCG
B2H-3273-R	AGATGGTACCCGCCACCTCAGCAGCCAGCGTCCC
B2H-3375-F	AGATTCTAGAGATGACGGTCGCGGAGACCATC
B2H-3375-R	AGATGGTACCCGCCCTAGCCCAAGGGCCTGCGG
B2H-3419-F	AGATTCTAGAGTTGAGCCGAGACCACGACAACTTC
B2H-3419-R	AGATGGTACCCGAACTCCATCGTCGGATCCCTC
B2H-3589-F	AGATTCTAGAGATGGTCGCGGAACAGGTCGG
B2H-3589-R	AGATGGTACCCGCCGCAAGGCGCTCAATCGCTC
CC-159-R-fuse-EC139	AGCAGATAGGTGATCGCTTCGAAGGTCAGGGCCGACTCGCAC
EC139-F	GAAGCGATCACCTATCTGCTGGAACAG
EC349-R	TTCTTCAATCTGCTGCAGTTTTTGCAG
CC-390-F-fuse-EC349	AACTGCAGCAGATTGAAGAAGAAACCGGCGTGCCGATCGAC
89Ec-F-XbAI	AGATTCTAGAGTCTGAAATCGGGCGCACGACTGAC
EC138-R	CGGATATTCAGCAACGGAGCATTGAAC
CC-160-F-fuseEC138	GCTCCGTTGCTGAATATCCGGAAGCCATCATGGTGTGGCGCG
389CCfuse350EC-R	TCGATGGTCAGGCCGGTTTCGGTGGCCAGGGCGGCGATCTCGC
350Ec-F	GAAACCGGCCTGACCATCGAGCAG
EC444-R-KpnI	AGATGGTACCCGCGCGATAGAGCGGGTGATCGCC
FB-ftsz-F	GGATGAGCCTCAGCGGCGTTCGG
FB-ftsZ-R	GGCCGGGGATGCCTCGACGATC
FB-mipz-F	GGACCAACGGGAACGCGTCCACAG
FB-mipz-R	GGACGACGATAACGCGCGTTTCGG
FB-ccka-F	GGAAAGAAGCCCCAGCCCCGG
FB-ccka-R	GGTTGTACCTTTCTTACGGCGAGCC
FB-ftsN-F-soe-T0AG6A	AACCTAGGGTCGCGCGCGTCAGATTCAATGCGTCGTTCCGTGCGCCGC
FB-mipZ-R-soe-mutants	TAATCGAAGGTTAACACGATGTTTCCCG
FB-mipZ-G3TG6A-T0GG6T	ATCGTGTTAACCTTCGATTAAGATTCACGGAGTCTCGACGCAGAAGGATCCGAG CCATG
FB-mipZ-A4T-G1C	ATCGTGTTAACCTTCGATTAAGAGACGCTCAGTCGCGACGCAGAAGGATCCG
FB-mipZ-R-soe-outside	GCGACCTTGGCGCCGCCGTACAG

R0059-F	CGGCGACAAAGTTGTTCAGT
R0059-R	TACCAAGGATGCGCTCTACC
R0021-F	CTGAAAAGGTCGTTGCATCC
R0021-R	CCAAAAACCGCAGTGTTACC
rpsL-F	AAGCCCGGAAGGAACGCAAG
rpsL-R	TTAACCGACGCGGGAACAGG
01305-F	AAGGCGCCTATCCAGAACC
01305-R	GTACGTTCCGGAATCGGTTT
ruvA-F	CGAGTGAGGAAGCCGTAGAG
ruvA-R	GACCCTGTTGCACATCGAG
Venus-F	ATGGTGAGCAAGGGCGAGGAGCTG
Venus-R-NheI	AGATGCTAGCTTACTTGTACAGCTCGTCCATGCCGAG
2236-F-HindIII	AGATAAGCTTTCCCAACATGGCGGGCTACAAG
2236-R-fuse-mipZ	GGACGCGTTCCCGTTGGTCCTCAGCGACAGAGGGTCTCCAGC
PmipZ-R-fuse-VENUS	TCCTCGCCCTTGCTCACCATGGCTCGGATCCTTCTGCGTCG

Table S7: ChIP-Seq strains and conditions

Strain	Genotype	Condition	Antibody
ML2297	Δ*gcrA(tet^R);* P$_{xyl}$*-gcrA-3xFLAG(kan^R)*	PYE + 0.3% xylose	Anti-FLAG (Sigma-Aldrich)
ML2296	Δ*gcrA(tet^R);* P$_{xyl}$*-gcrA(kan^R)*	PYE + 0.3% xylose	Anti-FLAG (Sigma-Aldrich)
ML2298	*gcrA::gcrA-3xFLAG(kan^R)*	PYE	Anti-FLAG (Sigma-Aldrich)
ML2299	*rpoC::rpoC-3xFLAG(kan^R)*	PYE	Anti-FLAG (Sigma-Aldrich)
ML2297	Δ*gcrA(tet^R);* P$_{xyl}$*-gcrA-3xFLAG(kan^R)*	PYE + 0.3% xylose + rifampicin 25 μg/mL for 30 min	Anti-FLAG (Sigma-Aldrich)
ML2299	*rpoC::rpoC-3xFLAG(kan^R)*	PYE + rifampicin 25 μg/mL for 30 min	Anti-FLAG (Sigma-Aldrich)
CB15N	Synchronizable wild-type CB15	PYE	Anti-FLAG (Sigma-Aldrich)
CB15N	Synchronizable wild-type CB15	PYE	Anti-RpoD (Neoclone)
CB15N	Synchronizable wild-type CB15	PYE + rifampicin 25 μg/mL for 30 min	Anti-RpoD (Neoclone)
ML2300	*rpoH::rpoH-3xFLAG(kan^R)*	PYE + rifampicin 25 μg/mL for 30 min	Anti-FLAG (Sigma-Aldrich)
ML2301	*rpoN::rpoN-3xFLAG(kan^R)*	PYE + rifampicin 25 μg/mL for 30 min	Anti-FLAG (Sigma-Aldrich)

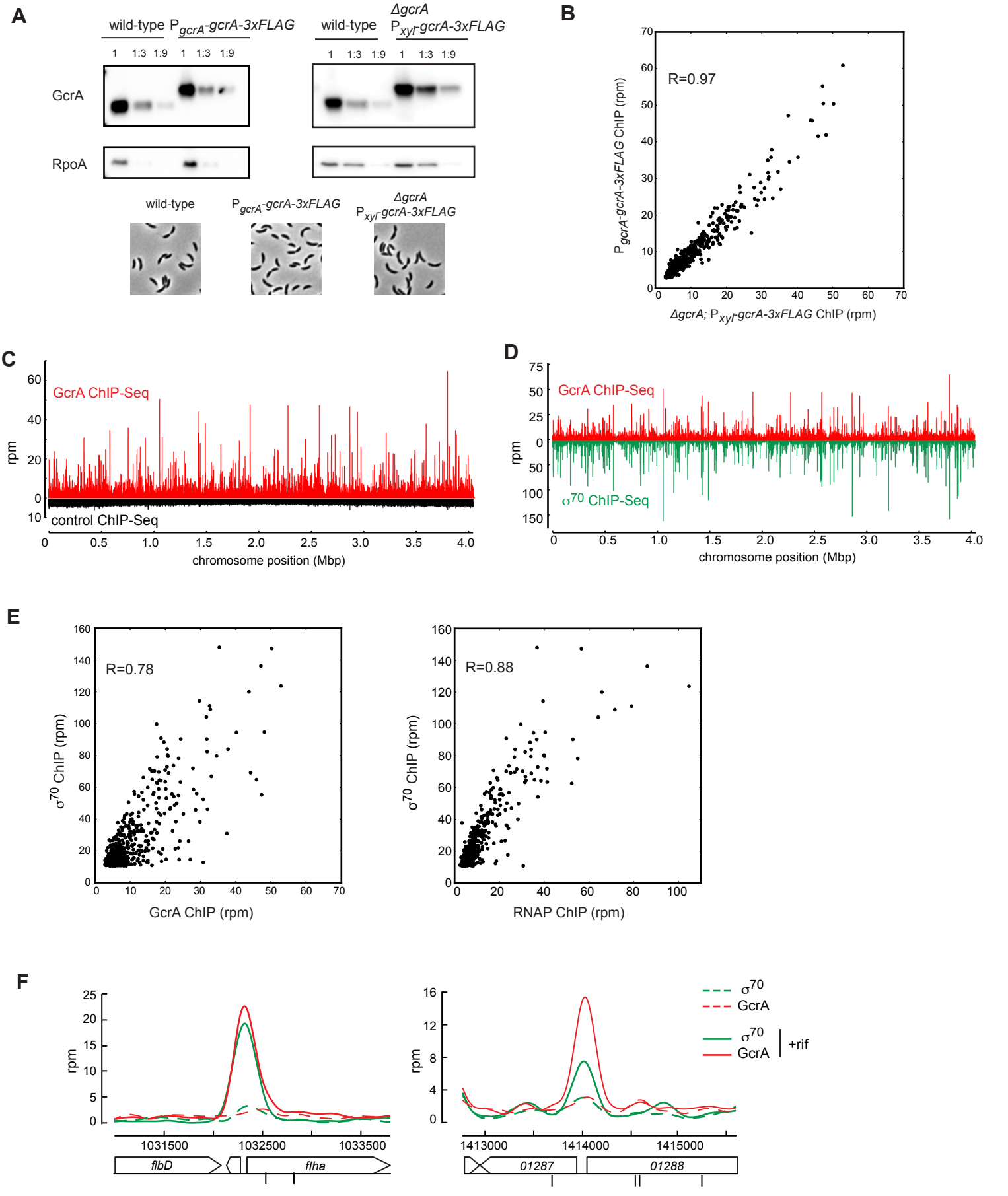
A
wild-type
P gcrA-gcrA-3xFLAG
wild-type
ΔgcrA
P xyl-gcrA-3xFLAG
1 1:3 1:9 1 1:3 1:9
1 1:3 1:9 1 1:3 1:9
GcrA
RpoA
wild-type
P gcrA-gcrA-3xFLAG
ΔgcrA
P xyl-gcrA-3xFLAG
B
R=0.97
P gcrA-gcrA-3xFLAG ChIP (rpm)
ΔgcrA; P xyl-gcrA-3xFLAG ChIP (rpm)
C
GcrA ChIP-Seq
control ChIP-Seq
rpm
chromosome position (Mbp)
D
GcrA ChIP-Seq
σ70 ChIP-Seq
rpm
chromosome position (Mbp)
E
R=0.78
σ70 ChIP (rpm)
GcrA ChIP (rpm)
R=0.88
σ70 ChIP (rpm)
RNAP ChIP (rpm)
F
rpm
1031500
1032500
1033500
flbD
flha
rpm
1413000
1414000
1415000
01287
01288
σ70
GcrA
σ70
GcrA
+rif

A

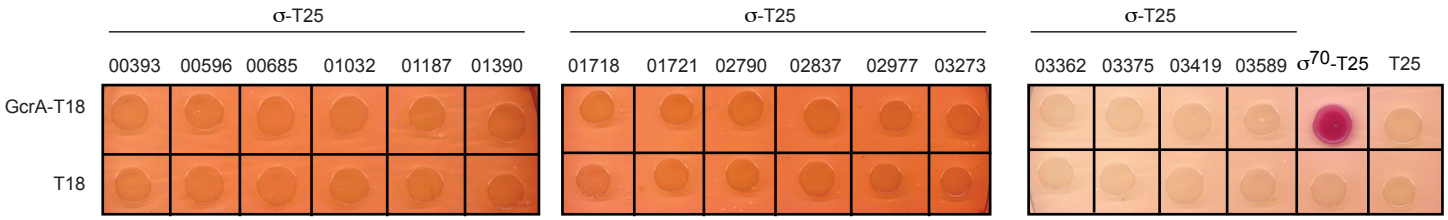
σ-T25
σ-T25
σ-T25
00393 00596 00685 01032 01187 01390
01718 01721 02790 02837 02977 03273
03362 03375 03419 03589 σ70-T25 T25
GcrA-T18
T18

B

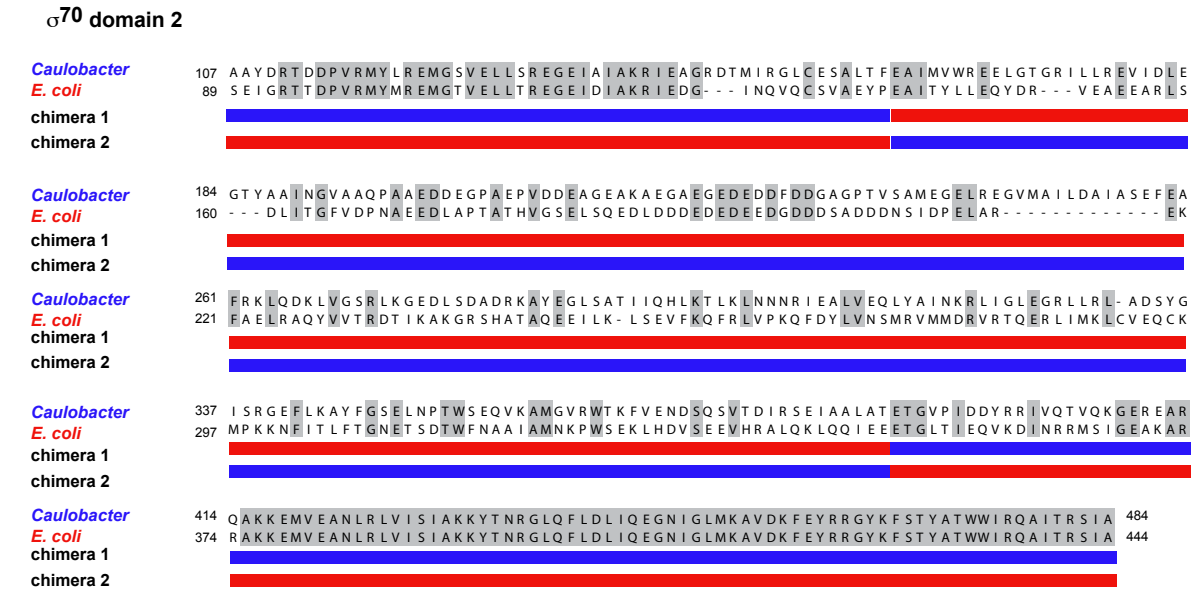
σ70 domain 2
Caulobacter
E. coli
chimera 1
chimera 2
107 AAYDRTDDPVRMYLREMGSVELLSREGEIAIAKRIEAGRDTMIRGLCESALTFEAIMVWREELGTGRILLREVIDLE
89 SEIGRTTDPVRMYMREMGTVELLTREGEIDIAKRIEDG---INQVQCSVAEYPEAITYLLEQYDR---VEAEEARLS
184 GTYAAINGVAAQPAAEDDEGPAEPVDDEAGEAKAEGAEGEDEDDFDDGAGPTVSAMEGELREGVMAILDAIASEFEA
160 ---DLITGFVDPNAEEDLAPTATHVGSELSQEDLDDDEDEDEEDGDDDSADDDNSIDPELAR----------EK
261 FRKLQDKLVGSRLKGEDLSDADRKAYEGLSATIIQHLKTLKLNNNRIEALVEQLYAINKRLIGLEGRLLRL-ADSYG
221 FAELRAQYVVTRDTIKAKGRSHATAQEEILK-LSEVFKQFRLVPKQFDYLVNSMRVMMDRVRTQERLIMKLCVEQCK
337 ISRGEFLKAYFGSELNPTWSEQVKAMGVRWTKFVENDSQSVTDIRSEIAALATETGVPIDDYRRIVQTVQKGEREAR
297 MPKKNFITLFTGNETSDTWFNAAIAMNKPWSEKLHDVSEEVHRALQKLQQIEEETGLTIEQVKDINRRMSIGEAKAR
414 QAKKEMVEANLRLVISIAKKYTNRGLQFLDLIQEGNIGLMKAVDKFEYRRGYKFSTYATWWIRQAITRSIA 484
374 RAKKEMVEANLRLVISIAKKYTNRGLQFLDLIQEGNIGLMKAVDKFEYRRGYKFSTYATWWIRQAITRSIA 444
chimera 1
chimera 2
σ70 Domain 2
C
N
Caulobacter
E. coli
100% identical
σ2-T25
Caulobacter E. coli chimera 1 chimera 2 T25
GcrA-T18
T18

C

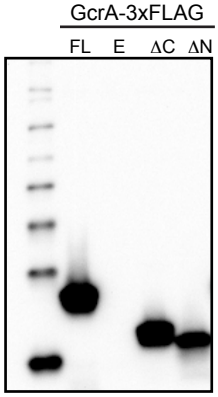
GcrA-3xFLAG
FL E ΔC ΔN

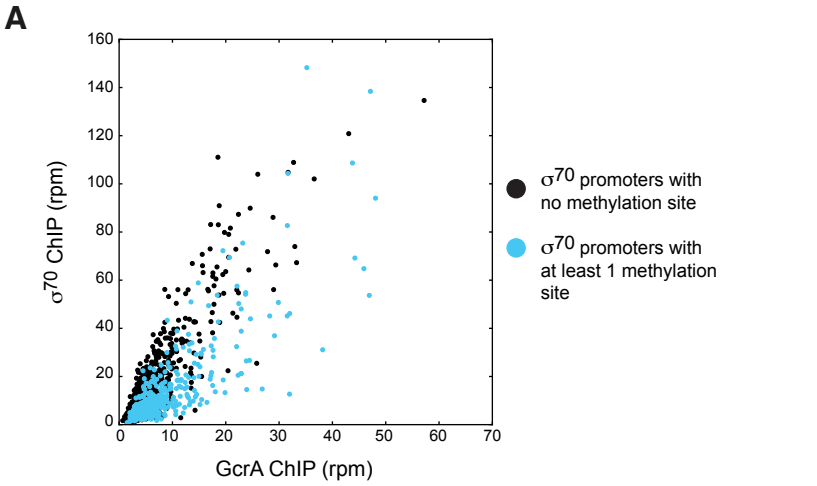

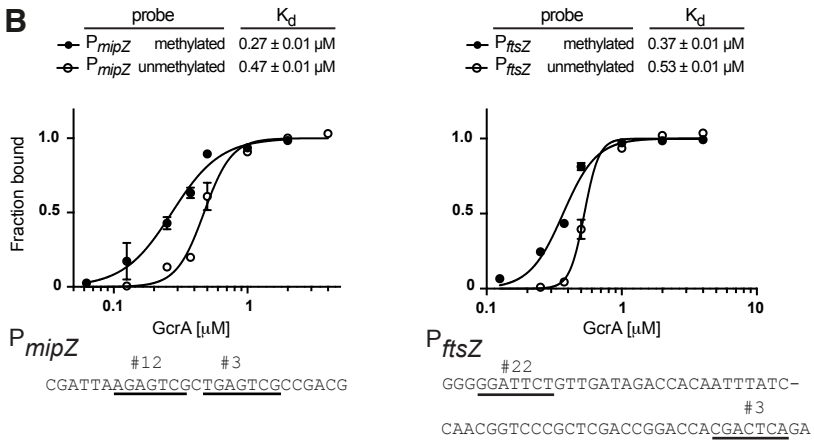

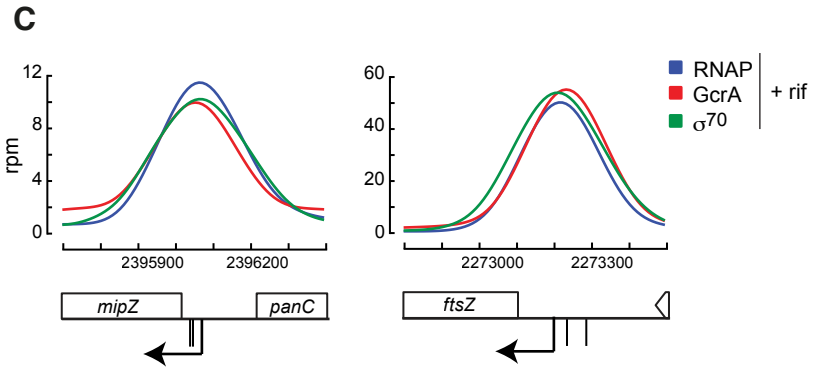

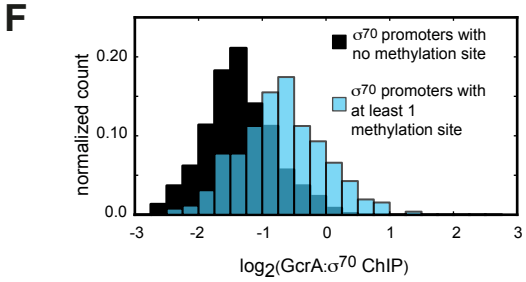

D

NGANTCN	Avg GcrA	rank
TGATTCG	6.697	1
CGATTCG	5.352	2
TGAGTCG	4.759	3
CGAGTCG	3.758	4
TGATTCT	3.519	5
CGATTCT	3.352	6
TGATTCC	3.203	7
TGAGTCT	2.976	8
AGATTCG	2.813	9
CGATTCC	2.759	10
CGATTCA	2.682	11
AGAGTCG	2.634	12
TGAGTCC	2.576	13
GGATTCG	2.412	14
CGAGTCT	2.384	15
TGATTCA	2.363	16
CGAGTCA	2.352	17
TGAGTCA	2.330	18
GGAGTCG	2.295	19
AGATTCT	2.271	20
CGAGTCC	2.241	21
GGATTCT	2.132	22
AGAGTCA	2.076	23
AGAGTCC	2.062	24
GGATTCC	2.016	25
AGAGTCT	2.013	26
GGAGTCC	2.011	27
GGAGTCA	1.942	28
TGTATCG	1.936	
AGATTCC	1.926	29
GGAGTCT	1.895	30
GGATTCA	1.856	31
AGATTCA	1.812	32

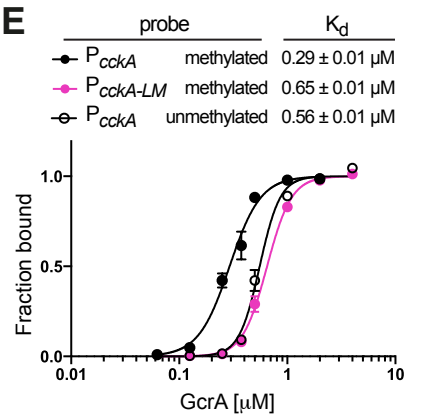

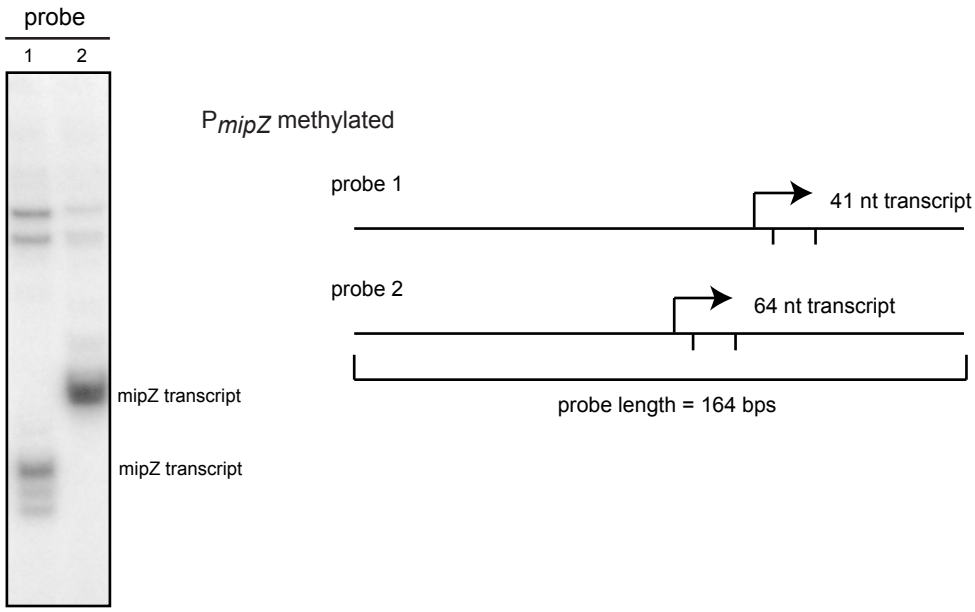
probe
1
2
mipZ transcript
mipZ transcript
P*mipZ* methylated
probe 1
41 nt transcript
probe 2
64 nt transcript
probe length = 164 bps

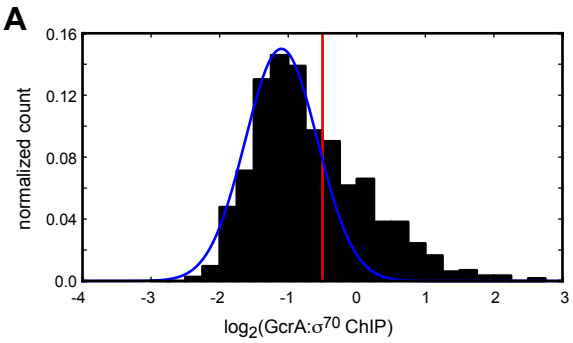
A
normalized count
0.16
0.12
0.08
0.04
0.0
-4
-3
-2
-1
0
1
2
3
log2(GcrA:σ70 ChIP)

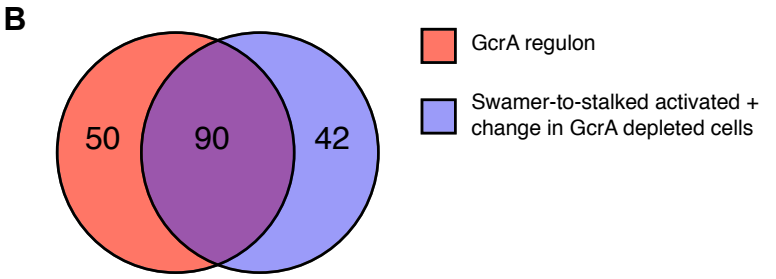
B
50
90
42
GcrA regulon
Swamer-to-stalked activated +
change in GcrA depleted cells

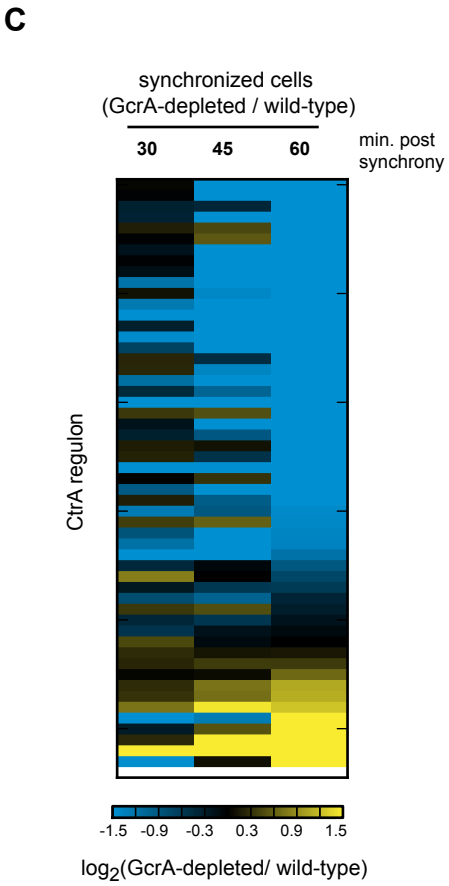
C
synchronized cells
(GcrA-depleted / wild-type)
30
45
60
min. post
synchrony
CtrA regulon
-1.5 -0.9 -0.3 0.3 0.9 1.5
log2(GcrA-depleted/ wild-type)

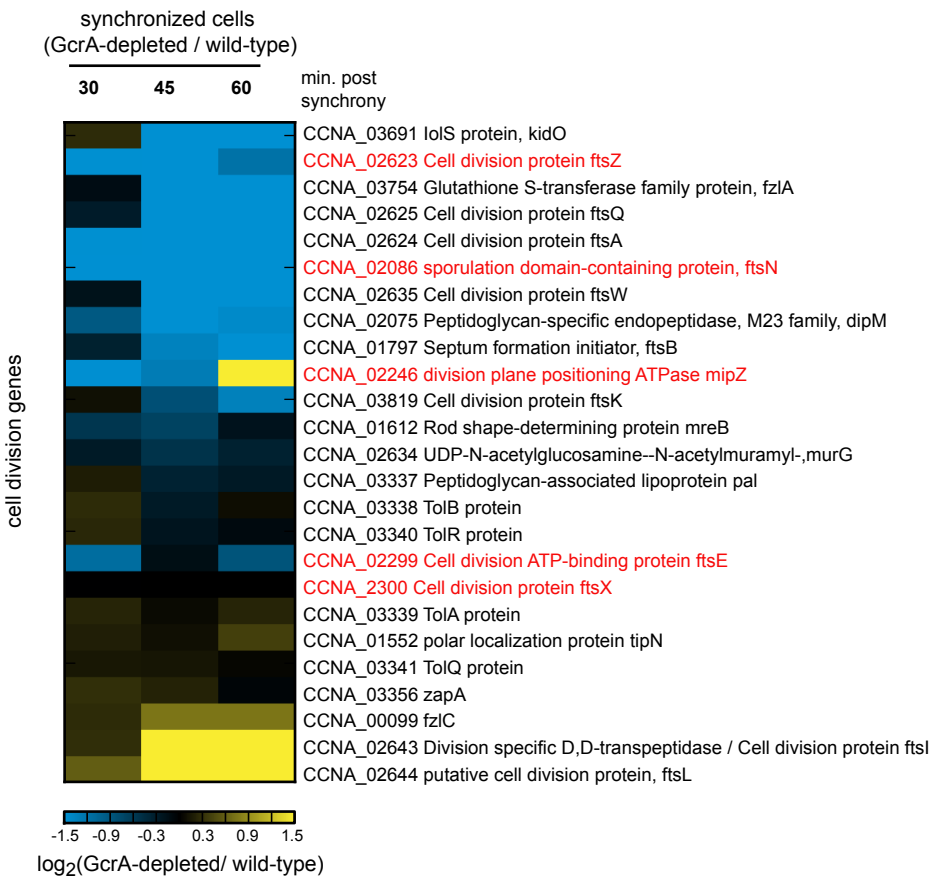
D
synchronized cells
(GcrA-depleted / wild-type)
30
45
60
min. post
synchrony
cell division genes
CCNA_03691 IolS protein, kidO
CCNA_02623 Cell division protein ftsZ
CCNA_03754 Glutathione S-transferase family protein, fzlA
CCNA_02625 Cell division protein ftsQ
CCNA_02624 Cell division protein ftsA
CCNA_02086 sporulation domain-containing protein, ftsN
CCNA_02635 Cell division protein ftsW
CCNA_02075 Peptidoglycan-specific endopeptidase, M23 family, dipM
CCNA_01797 Septum formation initiator, ftsB
CCNA_02246 division plane positioning ATPase mipZ
CCNA_03819 Cell division protein ftsK
CCNA_01612 Rod shape-determining protein mreB
CCNA_02634 UDP-N-acetylglucosamine--N-acetylmuramyl-,murG
CCNA_03337 Peptidoglycan-associated lipoprotein pal
CCNA_03338 TolB protein
CCNA_03340 TolR protein
CCNA_02299 Cell division ATP-binding protein ftsE
CCNA_2300 Cell division protein ftsX
CCNA_03339 TolA protein
CCNA_01552 polar localization protein tipN
CCNA_03341 TolQ protein
CCNA_03356 zapA
CCNA_00099 fzlC
CCNA_02643 Division specific D,D-transpeptidase / Cell division protein ftsI
CCNA_02644 putative cell division protein, ftsL
-1.5 -0.9 -0.3 0.3 0.9 1.5
log2(GcrA-depleted/ wild-type)

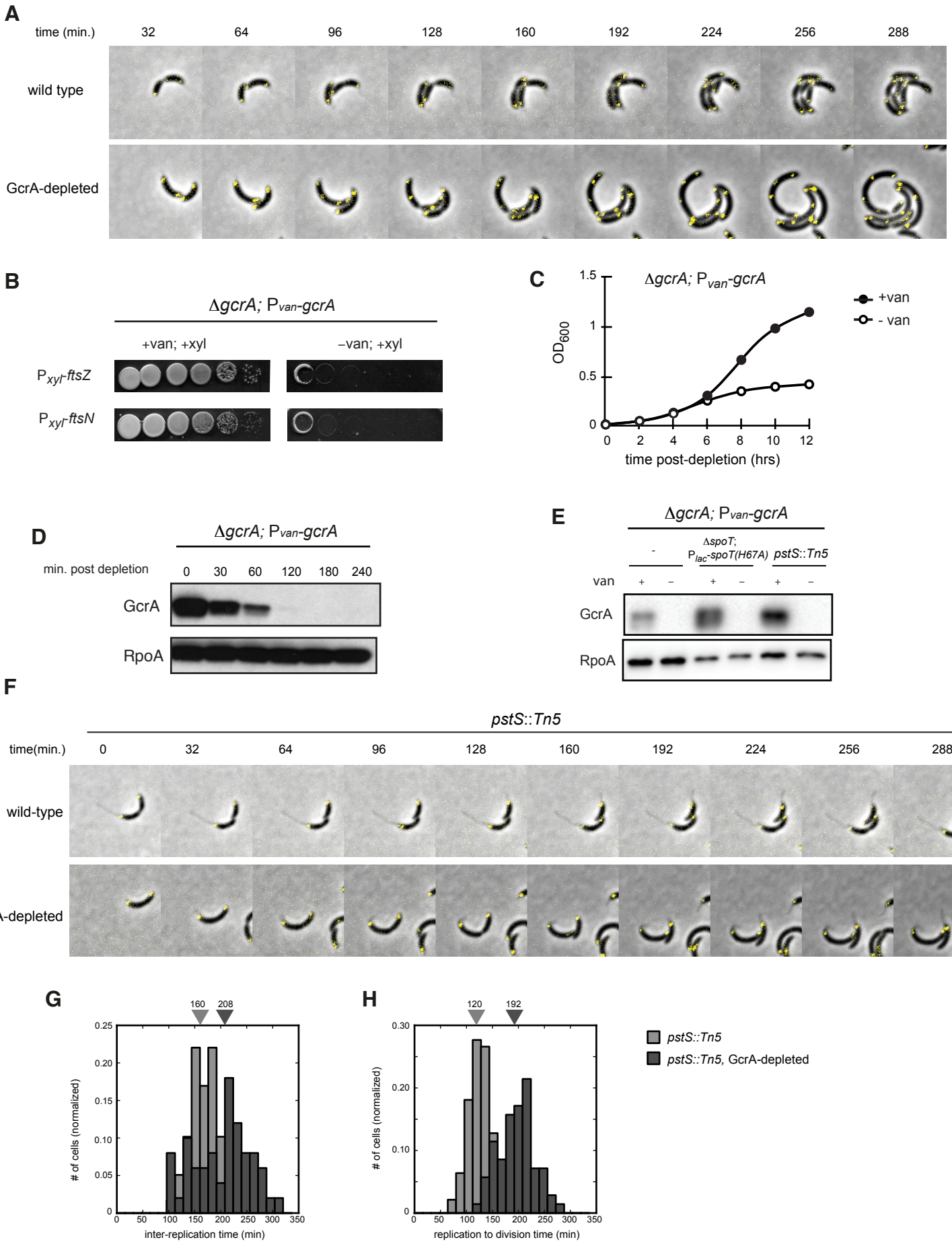
A
time (min.)
32
64
96
128
160
192
224
256
288
wild type
GcrA-depleted
B
ΔgcrA; Pvan-gcrA
+van; +xyl
–van; +xyl
Pxyl-ftsZ
Pxyl-ftsN
C
ΔgcrA; Pvan-gcrA
+van
- van
OD600
time post-depletion (hrs)
D
ΔgcrA; Pvan-gcrA
min. post depletion
0
30
60
120
180
240
GcrA
RpoA
E
ΔgcrA; Pvan-gcrA
-
ΔspoT; Plac-spoT(H67A)
pstS::Tn5
van
GcrA
RpoA
F
pstS::Tn5
time(min.)
wild-type
GcrA-depleted
G
160
208
# of cells (normalized)
inter-replication time (min)
H
120
192
# of cells (normalized)
replication to division time (min)
pstS::Tn5
pstS::Tn5, GcrA-depleted